Staffordshire Hoard Research Report 6

Pilot Study of Surface Enrichment in a Selection of Gold Objects from the Staffordshire Hoard

E. S. Blakelock

2013

This report forms part of
The Staffordshire Hoard: an Anglo-Saxon Treasure
edited by C. Fern, T. Dickinson and L. Webster
and published by the Society of Antiquaries of London

Information about this report

This report was produced in 2014 as part of Stage 1 of the project, i.e. before fragments were joined and catalogued. The concordance of the K numbers given in the report to the catalogue numbers as they appear in the final publication is as given below. The list also includes the names of the objects as used in the final publication.

The following article was based on this work.

Blakelock, E.S. Never judge a gold object by its surface analysis: a study of surface phenomena in a selection of gold objects from the Staffordshire Hoard, *Archaeometry* (doi: 10.1111/arcm.12209 - first published 5th October 2015).

K number	Catalogue number	Name in publication
3	336	Hilt-plate in gold (part).
10	325	Hilt-plate in gold.
12	261	Hilt-plate in gold with gemmed bosses (part).
79	329	Hilt-plate in gold (part).
95	488	Mount in gold with a forked end.
133	335	Hilt-plate in gold.
1048	295	Hilt-plate in gold.
1072	257	Hilt-plate in gold with a garnet boss.
1136	365	Hilt-plate in gold with garnet cloisonné trim and gemmed bosses.
1137	293	Hilt-plate in gold (part).
1143	330	Hilt-plate in gold.
1150	363	Hilt-plate in gold with garnet cloisonné (part).
1163	343	Hilt-plate in gold.
1221	313	Hilt-plate in gold.
1234	261	Hilt-plate in gold with gemmed bosses.
1272	46	Pommel in gold, of cocked-hat form, with garnet cloisonné decoration.

The British Museum

DEPARTMENT OF CONSERVATION AND SCIENTIFIC RESEARCH

Pilot study of surface enrichment in a selection of gold objects from the Staffordshire Hoard

Science Report PR07444-10

E. S. Blakelock

Abstract

Sixteen gold objects representing the known spatial distribution of the Staffordshire Hoard in the ground were selected by the Hoard Project Management for scientific analysis of the metal. It is well established that gold alloys can corrode and be altered by the loss of copper and small quantities of silver from their surfaces during burial, but it is also known that gold-smithing treatments carried out during manufacture may remove both copper and silver from the surface of gold alloys.

The aim of this study was to determine firstly whether there is any surface enrichment and/or depletion of the gold alloy that may affect future analysis programmes and secondly if this relates to the spatial distribution of the Hoard, as excavated. Finally, if there is significant but consistent surface alteration caused by the burial conditions, could this alteration be compensated for to give a close approximation to the actual alloy composition, thus allowing surface XRF to be used as a reliable tool for future analysis of the Staffordshire Hoard.

The degree of enrichment was assessed by comparing surface and sub-surface elemental compositions of the objects using both X-ray fluorescence (XRF) and scanning electron microscopy with energy dispersive X-ray analysis (SEM-EDX).

The results have clearly shown that in many of these items there is significant but not consistent enrichment of the gold at the surface due to the depletion of both copper and silver. The analysis of deep scrapes, probably made when dismantling the swords before burial, indicates the expected loss of copper from the surface during burial, and little loss of silver. However, the results from undamaged surfaces of the same objects show significant losses of silver, suggesting that some form of deliberately induced depletion gilding took place to remove both silver and copper from the surface. At this stage it is difficult to say whether this more sophisticated surface treatment was a widespread Anglo-Saxon metalworking practice. More work would need to be carried out on a larger range of object types, and particularly objects with multiple components to see whether they vary in composition and surface treatments.

All the above suggests that even XRF with its deeper penetration of the surface of the object can, at best, provide semi-quantitative data of the alloy composition.

CSR Project no. PR07444
March 2013
External Registration Numbers: Staffordshire Hoard K3, K10, K12, K79, K95, K133, K1048, K1072, K1136, K1137, K1143, K1150, K1163, K1221, K1234, K1272

Table of Contents

Figures and tables

Introduction

Staffordshire Hoard Pilot Project

This pilot study forms part of the first stage of the English Heritage-funded research and analysis project "Contextualising Metal-Detected Discoveries: Staffordshire Anglo-Saxon Hoard".[1] Sixteen objects were selected for this study by the Staffordshire Hoard project. They were excavated from the plough soil and were representative of the known spatial distribution of the hoard (Figure 1). These objects were also selected for their relatively plain design, with no or very little decoration and with few components (Figure 2). This reduces the risk that solder or fluxes will have altered the surface composition of the metal. Many of the pieces chosen were hilt plates.

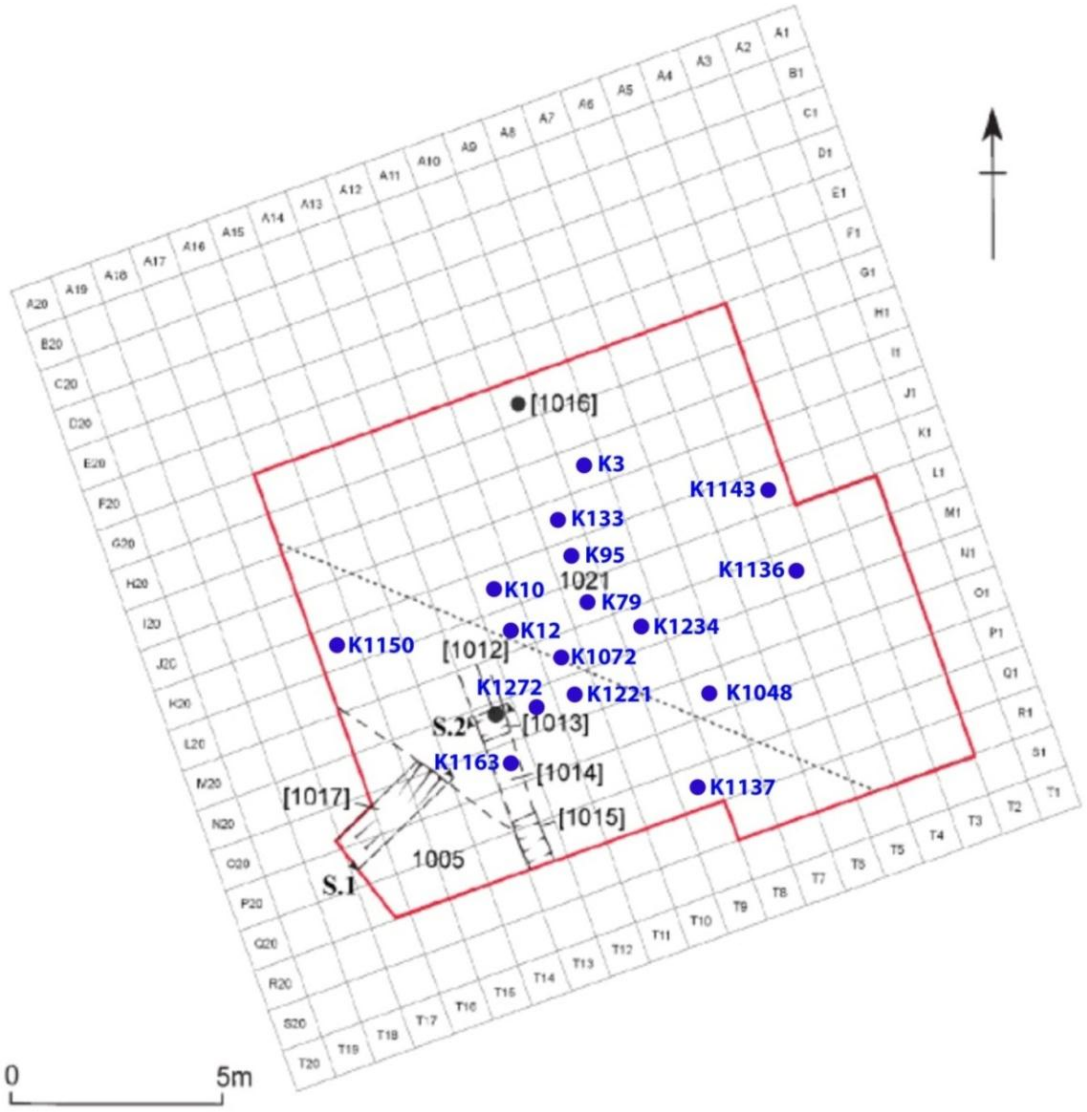

Figure 1. Spatial distribution of the Staffordshire Hoard objects selected for this pilot study. The dashed line shows where there was a change in subsoil, although all objects were found in the top 0.28 m in the plough soil.

[1] The Staffordshire Hoard is a large collection of Anglo-Saxon gold and silver metalwork. Discovered in a field near the village of Hammerwich, near Lichfield, in Staffordshire, England on 5 July 2009, it consists of more than 3,500 fragments, most of which appear to be from military fittings. For more information visit http://www.staffordshirehoard.org.uk/.

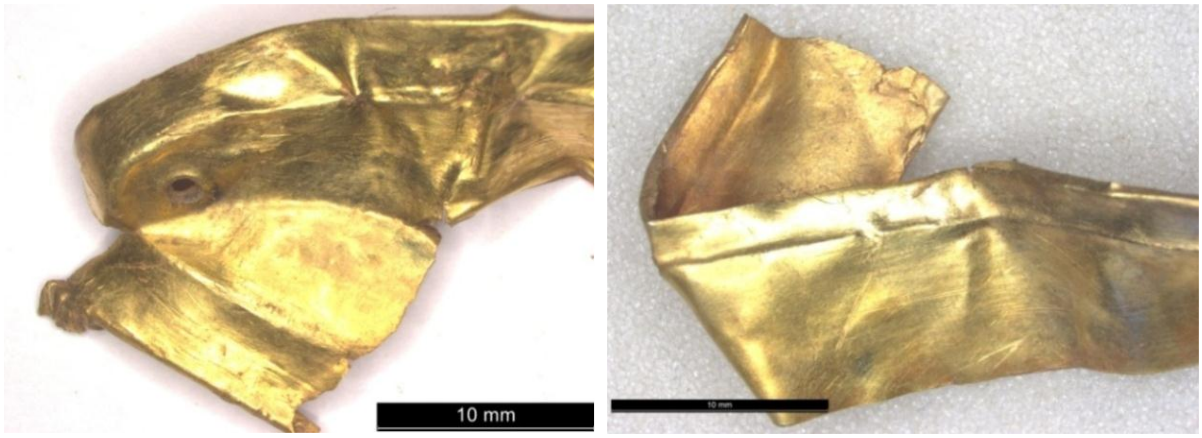

Figure 2. K3 on the left (scale bar 10 mm) and K1163 on the right (scale bar 10 mm). Like many of the hilt plates selected, they have been damaged, misshapen and/or folded in antiquity. Note the burnished front of K1163 compared to the matt back of the sheet visible at the top of the picture.

Most of the objects have a discernible back and front. There are two types of hilt plates in the selected assemblage. The first type appears to have been wrapped around a core, e.g. K3 (Figure 2 left) while the second consists of a flat plate once attached by riveting, e.g. K1234 and K1221 (Figure 3). Some of these pieces have filigree wire around the rivet holes (Figure 4). Both types of hilt plate have a visually obvious external surface that is often burnished and a matt internal surface. Prior to this study, the objects were partially conserved and, occasionally, this matt surface was not fully cleaned in order to preserve any organic remains potentially present, or to preserve in-situ foil fragments attached to the object. Only the burnished outer surface of the object would have been visible when the sword was in use. For these hilt plates, the external burnished and/or decorated surface will be referred to as the front and the internal matt and/or undecorated surface as the back. K95 appears to be a small fitting with nails on the back. Finally K1272 is a small fitting with two pins (Figure 5); this is the most complex piece in the group examined and is composed of a rectangular central panel with two cylinders holding gold pins attached to a thin sheet of gold on the back. Photographs of all the objects analysed are in appendix 1 of this report.

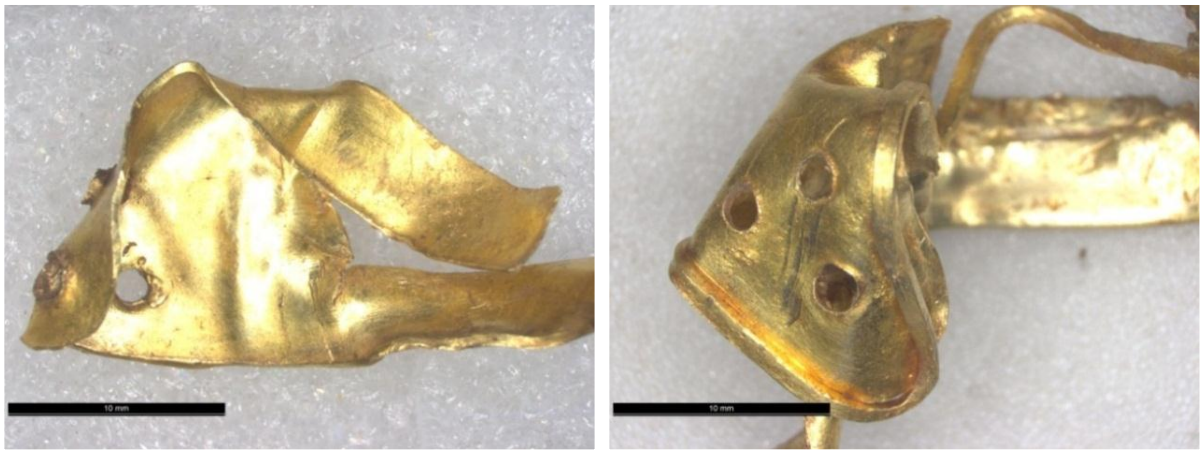

Figure 3. K1234 on the left (scale bar 10 mm) and K1221 on the right (scale bar 10 mm). Both are badly distorted, resulting in few flat areas suitable for analysis

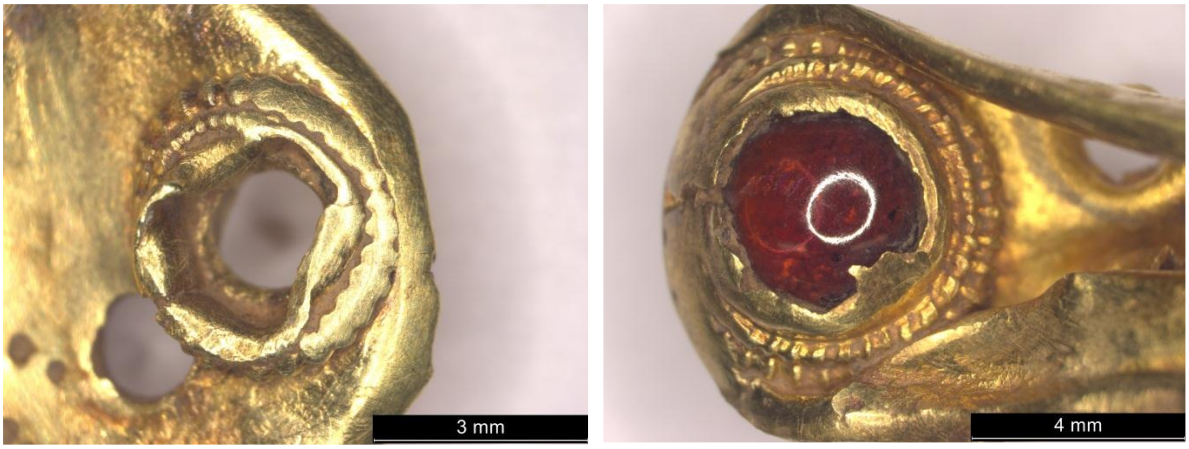

Figure 4. Gold filigree wire around one rivet hole on the front of K12 on the left (scale bar 3 mm) and cabochon garnet surrounded by filigree wire on the front of K1072 on the right (scale bar 4 mm).

Figure 5. Front and back of K1272.

Surface phenomena in gold alloys

Pure gold is very resistant to all forms of corrosion, including attack by acids and alkalis (Wise 1964), but most ancient gold is alloyed with silver and copper. In nature, alluvial gold, collected from river deposits, occurs with silver up to 40 wt%, but many sources have an average of 10 wt% silver and up to 1 wt% copper (Möller 1995; Raub 1995). As is the case with this group of objects, silver and/or copper were also deliberately added to change the properties of gold, including colour, melting temperature, ductility, hardness and tensile strength (Pingel 1995).

Tarnish is the product of a reaction between the surface of a metal and a non-metal compound in the environment which results in the formation of a thin layer on the surface (German 1981). Studies have shown that the degree of tarnishing decreases as the gold content of the alloy increases (Scott 1983b) but even alloys with gold contents above 92 wt% are susceptible to corrosion and tarnish (German 1981), and some experiments have shown that a gold content as high as 95 wt% may be necessary to prevent tarnishing problems occurring in contaminated environments (Wise 1948). Only two of the objects examined here

showed obvious tarnish: K133, which had much higher silver and lower gold contents than the other objects selected (see Table 1 on p.15), and K95 which has the appearance of having being exposed to heat post-manufacture (Figures 6 and 7).

Figure 6. K133 on the left (scale bar 6 mm) and K79 on the right (scale bar 10 mm) were particularly tarnished when compared to the other artefacts in this study.

Figure 7. Tarnished front of K79 on the left compared to the golden burnished front of K3 on the right.

Previous studies of ancient gold alloy objects have shown that there can be differences in copper and silver contents of up to 10 wt% between the surface and the core (Lehrberger and Raub 1995). In gold alloys, base metals, i.e. copper, can corrode and form soluble corrosion products which are leached away from the surface by the action of the burial environment. Copper as the least noble metal in these gold alloys is often found to be depleted at the surface (Hook and Needham 1989; Lehrberger and Raub 1995; Tate 1986; Voute 1995). Silver on the other hand is more resistant to corrosion. The chemical removal of silver from a gold alloy usually requires deliberate depletion, through methods like cementation or more recently through parting using mineral acids (Craddock 2000; La Niece 1995; Mongiatti *et al.* 2010). The result is a surface layer relatively enriched in gold (Lehrberger and Raub 1995; Scott 1983b; Voute 1995).[2]

[2] Some of these corrosion products can occasionally be re-deposited on the surface of the objects, for example Hoxne treasure (Cowell and Hook 2010), although the mechanism for this is not well understood.

X-ray fluorescence analysis (XRF) is one of the most common methods applied to the surface analysis of precious metals, due to its non-destructive nature and it is often hailed as the museum curators 'dream instrument' (Tate 1986), but the main disadvantage is the limited depth of penetration of the X-rays. Thus analytical data obtained by XRF is restricted to surface layers often only a few micrometres thick, i.e. 0.005-0.05 mm (Bachmann 1995; Cowell 1977; Cowell 1998; Hall 1961). Given that in some circumstances the depletion zone can be more than 0.1 mm thick (Hook and Needham 1989; Lehrberger and Raub 1995), surface analyses alone may not give the composition of the original alloy. Previous research has suggested that the results from surface analysis could be 10-15 wt% lower in silver and 30-40 wt% lower in copper than the core metal (Hook and Needham 1989).

Scanning electron microscopy-energy dispersive X-ray analysis (SEM-EDX) has a smaller depth penetration which allows the user to determine the superficial surface composition, and therefore identify any surface enrichment. It also has a smaller beam size and is able to analyse much smaller areas than the XRF.

Pilot project aims

The aim of this pilot study was to determine whether the artefacts from the Staffordshire Hoard exhibit surface enrichment in gold resulting from the loss of copper and silver from the original bulk gold alloy during burial and thus whether surface XRF could be used as a reliable indicator of bulk composition for future studies of this assemblage. The data was acquired using a combination of XRF and SEM-EDX, and the aim achieved by comparing data on elemental compositions on the surface of the objects with data from analysis of their sub-surface using SEM-EDX on small areas scraped through the surface using a micro-chisel.

Methodology

Equipment

The objects were examined using optical microscopy, XRF and SEM-EDX. The optical microscope was used to select areas for analysis by XRF and SEM-EDX.

The XRF instrument was a Bruker Artax spectrometer with a voltage of 50 kV and a current of 500 μA, using either a 0.65 mm or 0.2 mm collimator. The data were collected for 200 seconds with the 0.65 mm collimator and for 600 seconds with the 0.2 mm collimator. Energy to channel calibration on the XRF was performed using a pure silver standard prior to any analytical work.

The SEM used was a Hitachi S-3700N Variable Pressure SEM, used at high vacuum, set at an accelerating voltage of 20 kV and at an acquisition time of 150 seconds. Images were recorded in the Secondary Electron (SE) mode. The EDX compositional data were obtained using an Oxford Instrument INCA EDX microanalysis system with an INCAx-act Silicon Drift Detector (SDD). The SEM-EDX was calibrated using cobalt prior to any analytical work. Settings were a process time of 5, the dead time was *c.* 30% and the count rate was *c*. 9000 counts per second on the cobalt standard. Unless noted otherwise, the optimum working distance of 10 mm was used. Specific energy lines were selected in the SEM-EDX INCA software to calculate the quantity of each element present.

Equipment Parameters

A basic introduction to both XRF and SEM-EDX techniques is provided in appendix 2. The incident X-ray beam of the XRF instrument carries a higher energy than the incident electron beam of the SEM, which results in deeper penetration of the X-rays into the object when compared to the electrons of the SEM (Northover 1998). XRF and SEM-EDX analyses are both quantitative methods if the sample is homogeneous and if the surface is flat, clean and free of corrosion layers. Archaeological objects seldom match these pre-requisites so the results are therefore only qualitative or semi-quantitative (Stern 1995). Previous research has shown that surface analysis using the XRF will penetrate deeper than the SEM-EDX[3] but even so the results will not be quantitative as the fluorescent yield will come from the surface rather than the deeper core regions (Hall 1961; Hook and Needham 1989). Theoretically, 23% of the silver detected will derive from this depleted layer and this effect is greater for copper with between 74-95% of the total deriving from the depleted layer (Cowell 1977; Hook and Needham 1989), this is due to the smaller depth penetration for copper (0.007 mm rather than 0.12 mm for silver) (Hall 1961). Due to the complicated nature of the problem, it is impossible to accurately estimate using XRF the core composition of alloys where considerable surface enrichment has occurred (Hall 1961).

Various experiments were carried out using the XRF and SEM-EDX on gold standards or objects to show the potential factors affecting the analytical results. These are detailed in appendix 4 for XRF and appendix 5 for SEM-EDX. The two most relevant findings from these experiments are the effects of the XRF beam collimator size on the detection limits, and of the object geometry on the results for both XRF and SEM-EDX. The error produced using a smaller XRF 0.2 mm collimator with shorter count times (compared to the 0.65 collimator),[4] does not appear to be significant, especially for semi-quantitative surface analysis, although an acquisition time of 600 seconds produces more accurate results than 200 seconds. The geometry of the object does have an effect on the results, particularly where the analysed surface curves away from the detector. Generally the results from small changes in angle, up to 30º, still remain within one standard deviation of the average, and therefore are not likely to result in errors significant enough to influence semi-quantitative surface analysis. The geometry of the object in the SEM however showed that curved or tilted surfaces at angles ±30º (Figure 8) are likely to produce significantly increased errors, and hence the location of the detector in relation to the surface being analysed can significantly affect the results.

Standards and Quantification methods for the analytical data

A range of standards of known composition was analysed on each instrument to ensure that the results were comparable between them. The full results from this study are detailed in appendix 3. The standards analysed include the existing in-house made standards routinely used at the British Museum for XRF analysis and three externally made standards (MAC 1, 2 and 3) commissioned specifically for the Staffordshire Hoard project. In addition, every time the XRF instrument was used, standard SB8A was analysed to ensure that the data collected using the XRF were internally consistent (Table 6 in appendix 3). Similarly, to

[3] The XRF will penetrate up to 0.05 mm whereas the SEM-EDX can only penetrate 0.005 mm (Cowell 1998; Goldstein *et al.* 2003).

[4] A smaller collimator will reduce the number of counts and hence effect the detection limits.

check the internal consistency of the SEM, standard MAC2 was analysed regularly, usually on a weekly basis during the pilot (Table 7 in appendix 3)[5].

The XRF results were quantified using the Staffordshire Hoard high-gold method, except K133 for which the Staffordshire Hoard mid-gold method was used as described in appendix 3.The quantification of gold, silver and copper with the SEM-EDX Inca software was achieved using MAC2 for the standardisation process, as it had a comparable gold, silver and copper content to the majority of the Staffordshire Hoard artefacts analysed for this pilot project. See appendix 3 for more details about standardisation methods.

Enrichment Pilot Study Methodology

This section will be grouped by instrument, but there were three phases to the analysis. The first analysis phase carried out was surface XRF this allowed comparison with the SEM-EDX data but also informed the decision of how many SEM-EDX areas would be analysed in the next phase. The surface and subsurface analysis by SEM-EDX was then carried out. The final phase was the XRF sub-surface analysis of the areas prepared for the SEM-EDX.

XRF Surface Analysis

XRF analysis was performed on at least six different areas on each object, typically three on each side of the gold sheets, using the 0.65 mm collimator. Any areas of filigree decoration on the front of the objects were avoided to reduce the risk of contamination from any solders used. On the back of the objects, relatively clean areas were chosen for analysis wherever possible to avoid contamination. For example, K133 still had possible organic remains and a fragment of silver foil adhering to the surface so the back of this hilt plate was intentionally not fully cleaned, but it was still possible to analyse two clean areas and one semi-cleaned area. As mentioned above, to obtain the most accurate data it was important to optimise the geometry of the surface to be analysed in relation to the detector, which meant that some samples therefore had to be suitably supported and positioned underneath the XRF beam to provide horizontal flat surfaces for analysis.

Following the SEM-EDX sub-surface analysis (see below) the effect of the surface enrichment on the XRF results was assessed by analysing the same cleaned sub-surface areas used in the SEM-EDX. This was carried out using the XRF instruments 0.2 mm collimator as the beam size of the 0.65 mm collimator was too large to analyse these small subsurface areas. In each case, a surface area beside each sub-surface area was analysed using the 0.2mm collimator to allow direct comparison.

SEM-EDX Analysis

For many of the objects, surface XRF showed that there was little variation in composition across a single object but XRF revealed that five objects had noticeable differences between the front and back of the object often with higher gold on the front side than the back (K10, K133, K1136, K1143 and K1221). These results, combined with time and geometry constraints (see below and appendix 5), led to the decision to analyse only one area on each object using SEM-EDX. The surface areas selected were relatively flat and easy to orient within the SEM vacuum chamber at the optimum working distance of 10 mm from the SEM-EDX detector. Any areas with obvious superficial surface debris were avoided.

[5] The two different standards (SB8A and MAC2) were used to compare the internal consistency of the instrument, both were analysed by XRF and SEM-EDX as part of the cross comparison between the techniques in appendix 3.

The surface areas analysed were then locally wiped with industrial methylated spirits (IMS) and analysed again. This solvent cleaning does not alter the chemical composition of the metal but removes any superficial dirt and grease from the surface and may also remove some corrosion products accumulated on the surface of the object (Araújo *et al.* 1993; Kallithrakas-Kontos and Katsanos 1998).

The extent of surface enrichment in gold (and depletion in copper and silver) was measured through the analysis of small sub-surface areas. These sub-surface areas were accessed by scraping the surface of the objects. This was carried out using a small tool under the optical microscope. The tool was sharpened to a chisel with an edge of less than 0.2 mm (Figure 8). The scraped areas are usually not larger than 1 mm^2 (Figure 9). This scraping of the surface to reveal the sub-surface was particularly important with tarnished artefacts (Figures 6 and 7), but as discussed above even where the surface was not obviously tarnished, surface depletion can occur. These small sub-surface areas were repeatedly analysed and scraped deeper until no further changes in composition occurred, indicating that the core alloy composition had been obtained. At each sub-surface depth, three or four analyses were carried out and the average composition calculated.

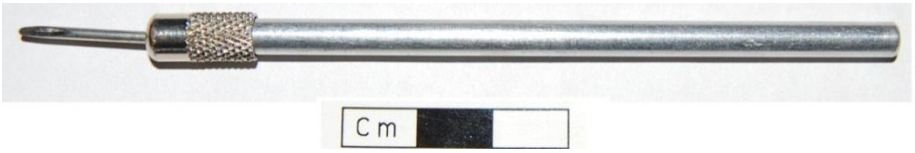

Figure 8. Tool used to scrape the surface to reveal the sub-surface.

Figure 9. Back of K1221 (scale bar 1 mm) showing deep old scrapes on the left of the scale bar, with an orange-yellow patina similar to that seen on the rest of the surface. Above and to the right of the scale bar (black arrow) is one of the areas (*c.*1 mm^2) scratched down to the brighter core metal for sub-surface analysis. The red arrow shows a second smaller and shallower scratched area that was analysed to check the initial results from the first area

On some objects, genuine old scrapes on the surface which had the same patina as the rest of the object surface suggest damage which had occurred before burial. So when it was possible, i.e. when a suitable flat area was available, the opportunity was taken to analyse these for comparison with the surface and sub-surface analyses (Figure 9).

Results

The results from XRF surface analysis show that the composition of the objects selected for the enrichment study are generally about 70-85 wt% gold, 14-28 wt% silver, and 1-2 wt% copper (Table 1 and Figure 10). The two exceptions are: K95, which is a high gold alloy (with *c*. 98 wt% Au, 1-1.5 wt% Ag and 0.5 wt% Cu) and K133, which is a base gold alloy (with *c*. 45-50 wt% Au, 45-50 wt% Ag and 1.5-2.7% Cu). Generally the gold content of the burnished front of each object is higher or equal to that of the back.

		Front			Back		
Object		**Wt% Au**	**Wt% Ag**	**Wt% Cu**	**Wt% Au**	**Wt% Ag**	**Wt% Cu**
K3	Average	82.2	15.6	2.2	83.5	14.8	1.7
	Standard Deviation	***0.61***	***0.50***	***0.15***	***0.70***	***0.35***	***0.35***
K10	Average	82.4	15.9	1.7	83.6	15.1	1.3
	Standard Deviation	***0.32***	***0.17***	***0.15***	***0.21***	***0.26***	***0.06***
K12	Average	78	19.5	2.5	77.4	17.6	5
	Standard Deviation	***0.94***	***0.57***	***0.58***	***1.37***	***1.08***	***2.30***
K79	Average	75.8	22.9	1.3	76.3	22.6	1.1
	Standard Deviation	***1.30***	***0.89***	***0.42***	***0.31***	***0.21***	***0.09***
K95	Average	98.1	1.6	0.4	98.2	1.3	0.6
	Standard Deviation	***0.13***	***0.15***	***0.01***	***0.42***	***0.07***	***0.38***
K133	Average	52.9	45.6	1.5	49.1	48.7	2.2
	Standard Deviation	***1.10***	***1.07***	***0.18***	***0.21***	***0.10***	***0.11***
K1048	Average	78.2	19.5	2.3	78.7	19.7	1.7
	Standard Deviation	***0.17***	***0.24***	***0.32***	***0.74***	***0.74***	***0.14***
K1072	Average	81.4	17.1	1.4	80.8	17.9	1.3
	Standard Deviation	***1.24***	***0.91***	***0.33***	***1.06***	***0.86***	***0.23***
K1136	Average	79.4	18.6	1.9	76.1	22.6	1.3
	Standard Deviation	***0.42***	***0.34***	***0.16***	***0.39***	***0.46***	***0.38***
K1137	Average	74.5	23.4	2.1	72.7	25.5	1.8
	Standard Deviation	***2.53***	***2.20***	***1.00***	***0.16***	***0.18***	***0.02***
K1143	Average	84.6	14.1	1.3	82.2	15.9	1.9
	Standard Deviation	***1.31***	***0.93***	***0.40***	***1.07***	***1.05***	***0.19***
K1150	Average	82.9	15.5	1.6	79.7	15.1	5.2
	Standard Deviation	***0.28***	***0.25***	***0.15***	***2.11***	***1.02***	***1.52***
K1163	Average	74	24	2	74.2	24.3	1.5
	Standard Deviation	***0.95***	***0.50***	***0.96***	***0.52***	***0.34***	***0.22***
K1221	Average	70.2	27.2	2.7	68.2	30.3	1.5
	Standard Deviation	***1.53***	***1.89***	***0.37***	***1.11***	***0.95***	***0.16***
K1234	Average	79.8	18.4	1.8	79.3	19.2	1.5
	Standard Deviation	***1.14***	***1.15***	***0.36***	***0.61***	***0.63***	***0.08***
K1272	Average	82.9	15.3	1.9	82.6	15.5	1.9
	Standard Deviation	***0.22***	***0.20***	***0.07***	***0.06***	***0.08***	***0.03***

Table 1. XRF results from the surface analysis of the Staffordshire Hoard objects chosen for the enrichment pilot study. The results are normalised and calculated from an average of at least three areas across the object.

SEM-EDX analysis (Table 2) of the surface of most items, both before and after cleaning with IMS, revealed a wider range of compositions from 70-93 wt% gold, 8-29 wt% silver, and up to 2.6 wt% copper but mostly between 0.5-1.5 wt% copper, with the exception of the high gold alloy K95 and base gold alloy K133 mentioned above.

The SEM-EDX sub-surface analysis by comparison revealed compositions mostly in the range of 70-85 wt% gold, 14-28 wt% silver and 2-4 wt% copper. There were two noticeable exceptions, K95 (*c.* 97-98 wt% Au, 1.5-2.5 wt% Ag, 0.4 wt% Cu) and K133 (*c.* 47-48 wt% Au, 50-51 wt% Ag, 2 wt% Cu).

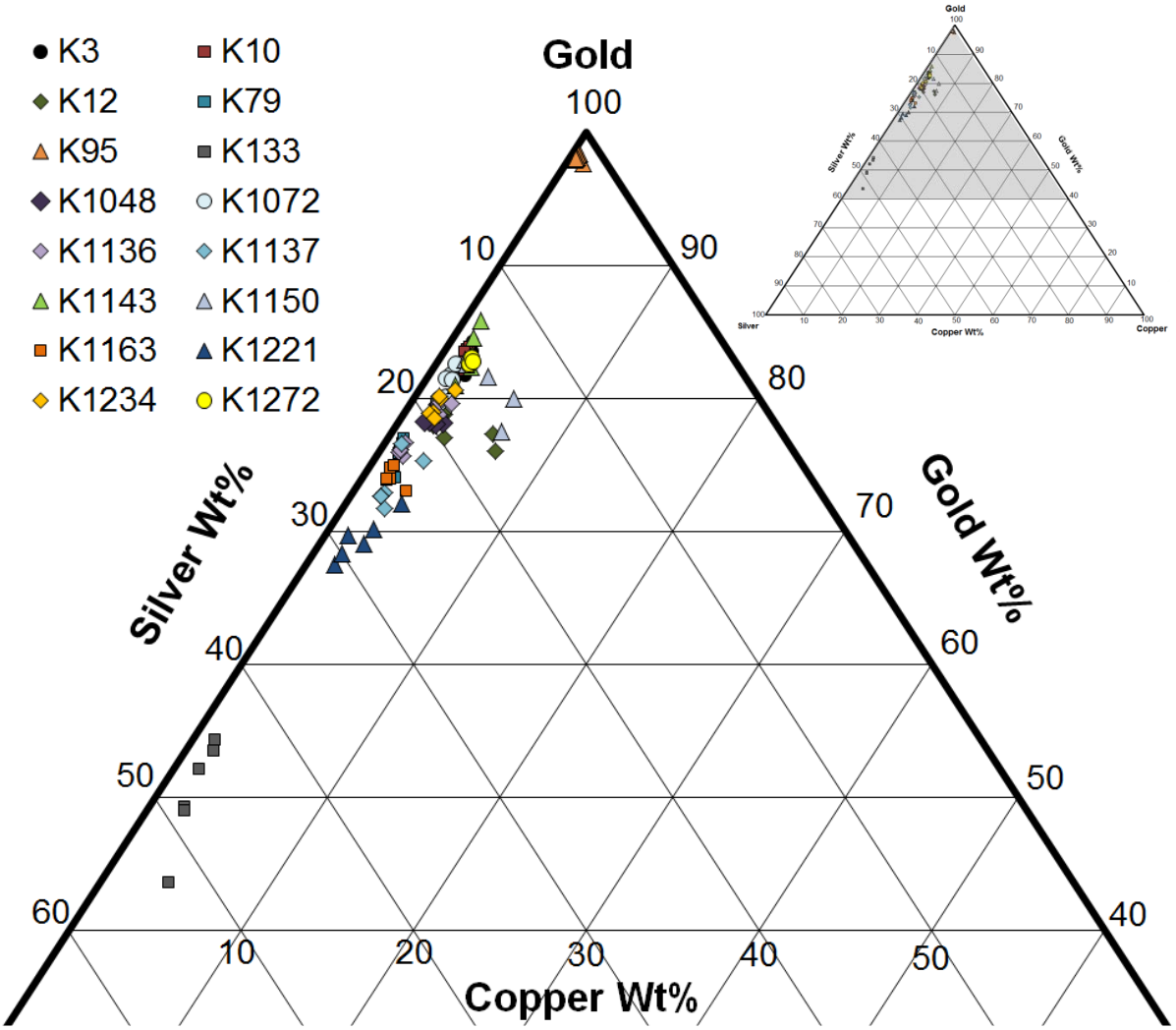

Figure 10. Part of a ternary gold-silver-copper diagram displaying all the surface data collected by XRF for all sixteen objects

Comparison of the surface and subsurface SEM-EDX compositions show that the objects can be divided into two groups (Table 2). The first group consists of artefacts K79, K1136 and K1143, which have the expected depletion in copper the most base metal of the alloy, associated with burial, and therefore a slight enrichment in gold and silver. The second and larger group of artefacts includes K3, K10, K12, K1048, K1072, K1137, K1150, K1163, K1221, K1234 and K1272, and shows an increase in the gold content at the surface, due to the depletion in both silver and copper. In several artefacts, namely K3, K10, K12, K1150, K1221 and K1234, there is almost a 40-50% depletion of silver at the surface.

One of the two outliers, K133, appeared to have no depletion of either silver or copper at the surface. The second K95 has a much higher gold content than the other objects analysed in this pilot study and has an apparent enrichment in silver at the surface. These differences in silver concentrations may indicate variation within the object itself rather than a surface phenomenon.

		Surface			Surface cleaned with IMS			Sub-surface		
Object		Wt% Au	Wt% Ag	Wt% Cu	Wt% Au	Wt% Ag	Wt% Cu	Wt% Au	Wt% Ag	Wt% Cu
K3	Average	90.9	8.1	1.1	89.7	9.4	0.9	81.6	15.7	2.6
	Standard Deviation	***1.18***	***0.96***	***0.22***	***0.29***	***0.21***	***0.14***	***0.99***	***0.94***	***0.15***
K10	Average	88.6	10.4	1.0	91.5	8.0	0.5	82.8	14.9	2.3
	Standard Deviation	***2.43***	***1.92***	***0.54***	***0.20***	***0.21***	***0.04***	***1.05***	***1.07***	***0.06***
K12	Average	86.5	12.4	1.2	85.8	13.2	1.0	77.5	20.2	2.3
	Standard Deviation	***0.15***	***0.09***	***0.11***	***0.30***	***0.33***	***0.08***	***1.00***	***0.83***	***0.38***
K79	Average	70.0	29.2	0.8	71.9	26.9	1.1	72.0	26.4	1.7
	Standard Deviation	***1.36***	***1.39***	***0.08***	***2.36***	***2.55***	***0.40***	***0.82***	***0.77***	***0.19***
K95	Average	96.6	3.1	0.3	96.5	3.2	0.3	97.9	1.7	0.4
	Standard Deviation	***0.12***	***0.08***	***0.10***	***0.06***	***0.08***	***0.03***	***0.15***	***0.11***	***0.04***
K133	Average	48.6	49.3	2.2	47.8	49.9	2.3	47.2	50.4	2.3
	Standard Deviation	***1.01***	***0.98***	***0.22***	***2.27***	***2.29***	***0.16***	***0.67***	***0.60***	***0.09***
K1048	Average	83.2	15.2	1.6	83.4	15.0	1.6	80	17.9	2.1
	Standard Deviation	***0.23***	***0.18***	***0.08***	***0.52***	***0.51***	***0.09***	***0.38***	***0.40***	***0.08***
K1072	Average	81.7	17.5	0.8	81.8	17.4	0.8	78.6	19.7	1.7
	Standard Deviation	***0.84***	***0.84***	***0.06***	***0.73***	***0.66***	***0.17***	***0.45***	***0.42***	***0.08***
K1136	Average	77.2	21.6	1.2	77.1	21.9	1.0	76.6	20.8	2.7
	Standard Deviation	***0.52***	***0.69***	***0.18***	***0.55***	***0.70***	***0.15***	***0.81***	***0.76***	***0.06***
K1137	Average	75.2	23.7	1.1	74.8	24.0	1.2	71.8	26.0	2.2
	Standard Deviation	***0.42***	***0.46***	***0.04***	***0.38***	***0.44***	***0.09***	***0.66***	***0.47***	***0.23***
K1143	Average	85.5	13.5	1.0	85.1	13.7	1.2	83.2	14.6	2.3
	Standard Deviation	***0.79***	***0.68***	***0.16***	***0.63***	***0.56***	***0.17***	***0.41***	***0.28***	***0.14***
K1150	Average	92.8	6.3	0.9	92.4	6.7	1.0	82.2	15.9	1.9
	Standard Deviation	***0.60***	***0.57***	***0.07***	***0.45***	***0.44***	***0.08***	***0.32***	***0.33***	***0.06***
K1163	Average	81.0	17.7	1.3	80.9	17.1	1.9	74.3	23.5	2.2
	Standard Deviation	***0.35***	***0.23***	***0.13***	***0.34***	***0.60***	***0.49***	***0.69***	***0.28***	***0.44***
K1221	Average	83.8	15.3	0.9	84.2	14.6	1.3	69.2	28.2	2.6
	Standard Deviation	***1.16***	***1.21***	***0.13***	***0.57***	***0.52***	***0.11***	***1.04***	***1.31***	***0.30***
K1234	Average	87.6	11.5	0.9	88.4	10.7	0.9	79.8	18.1	2.1
	Standard Deviation	***0.57***	***0.53***	***0.04***	***0.43***	***0.40***	***0.05***	***1.31***	***1.23***	***0.09***
K1272	Average	84.5	13.6	1.9	84.5	13.2	2.4	80.7	15.1	4.1
	Standard Deviation	***0.40***	***0.40***	***0.04***	***0.69***	***0.60***	***0.24***	***0.32***	***0.40***	***0.32***

Table 2. SEM-EDX surface and sub-surface compositions. The results are normalised and calculated from an average of at least six different areas.

Table 3 presents the results from the XRF analysis of the sub-surface areas previously analysed by SEM_EDX and compares it with the surface composition. It shows that the XRF analysis of the sub-surface with the small 0.2 mm collimator provides a better correlation with EDX analysis of the sub-surface than surface XRF analysis, particularly for the copper concentration.

The results in table 2 and 3 showed that the use of IMS to clean the objects prior to analysis often had little effect on the concentrations detected on the surface of the object. It did however remove any remaining grease and superficial dirt resulting in cleaner areas for analysis.

	XRF surface cleaned with IMS			XRF sub-surface			SEM sub-surface		
Object	Wt% Au	Wt% Ag	Wt% Cu	Wt% Au	Wt% Ag	Wt% Cu	Wt% Au	Wt% Ag	Wt% Cu
K3	81.6	16.3	2.1	82.1	15.5	2.4	81.6	15.7	2.6
K10	83.1	15.6	1.3	82	15.8	2.2	82.8	14.9	2.3
K12	78.7	19.2	2.1	78.5	19.3	2.1	77.5	20.2	2.3
K79	76.3	22.6	1.1	75.1	23.4	1.5	72.0	26.4	1.7
K95	98.2	1.5	0.4	98.2	1.4	0.4	97.9	1.7	0.4
K133	49.3	48.7	2	47.8	49.9	2.3	47.2	50.4	2.3
K1048	79.3	18.9	1.8	79.2	19.0	1.9	80.0	17.9	2.1
K1072	80.9	17.8	1.4	80.1	18.4	1.5	78.6	19.7	1.7
K1136	79.1	18.7	2.3	78.3	19.1	2.6	76.6	20.8	2.7
K1137	72.7	25.4	1.9	72.6	25.4	2.0	71.8	26.0	2.2
K1143	83.1	15.3	1.5	82.0	16.0	2.0	83.2	14.6	2.3
K1150	83.6	14.9	1.4	83.9	14.4	1.7	82.2	15.9	1.9
K1163	74.9	23.2	1.9	73.4	23.9	2.7	74.3	23.5	2.2
K1221	69.5	28.3	2.2	67.7	30.0	2.4	69.2	28.2	2.6
K1234	79.0	19.3	1.6	79.1	19.4	1.6	79.8	18.1	2.1
K1272	80.1	16.4	3.5	80.8	16.2	2.9	80.7	15.1	4.1

Table 3. XRF surface and sub-surface compositions using the 0.2 mm collimator, compared to the SEM-EDX sub-surface results which are the average of at least three areas. The results are normalised.

Discussion

The full set of surface and sub-surface compositional data for each hilt plate from both the XRF and SEM-EDX is presented in appendix 1. For each object, two plots have also been included, silver concentrations are plotted against copper concentrations and gold concentrations respectively, showing the results of the different types of analysis.

The results clearly demonstrate the difference between the two methods as a result of the greater energy and penetration of the X-rays produced by the XRF instrument compared to the electrons of the SEM which cannot penetrate more than 0.005 mm below the surface (Northover 1998; Verma 2007). Because of this the surface XRF results are more comparable to the sub-surface composition identified by SEM-EDX. Even so the XRF results show a trend to a slightly lower silver concentration, and often a significant difference between copper concentrations as although the beam penetrates deeper into the core, the corroded surface layers still contribute to the total signal measured (Cowell 1998; Hall 1961; Tate 1986). Sub-surface XRF analyses carried out on the areas prepared for sub -surface SEM-EDX analysis showed better agreement between the two methods, particularly with regards to the copper concentration. Thus it was obviously necessary to carry out sub-surface analysis to accurately determine the core metal composition for these gold objects.

Majority of the objects

The majority of the object surfaces, (with the exception of the two outliers, K95 and K133, identified above), display an apparent enrichment in gold because of silver and/or copper depletion. This is clearly shown by the silver/copper and silver/gold concentration plots in appendix 1 and illustrated by the example below in Figure 11 for K3

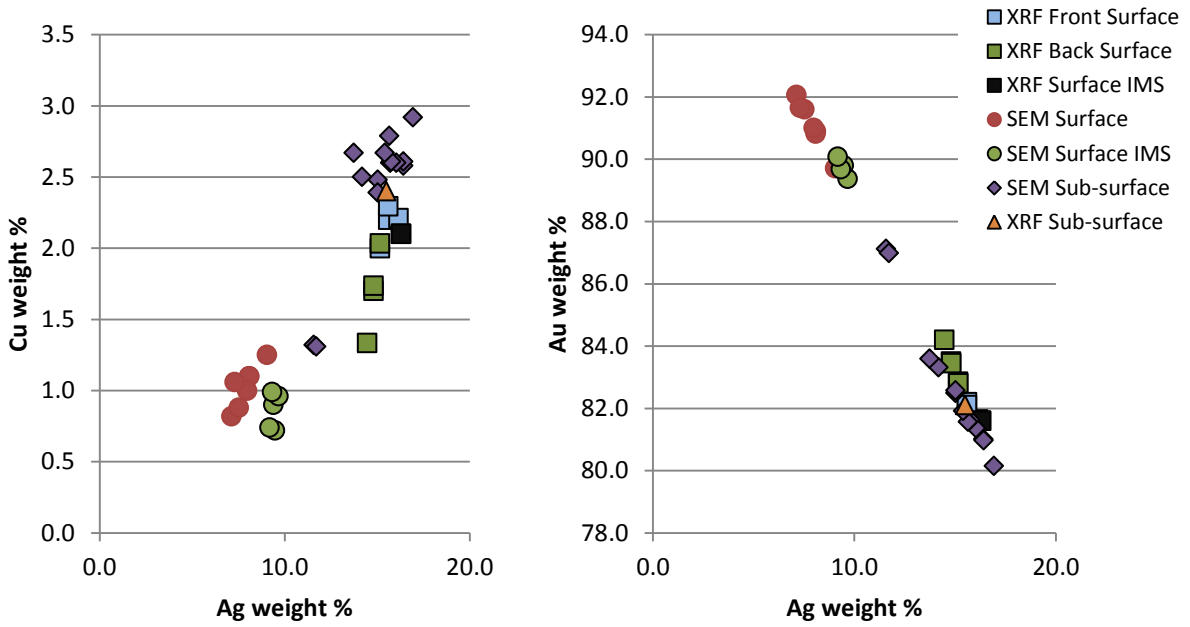

Figure 11. Silver/copper (left) and silver/gold (right) concentration plots of the XRF and SEM-EDX data for K3 showing the differences between the sub-surface and surface analyses.

The sub-surface and surface analyses of a typical example from the pilot group (K1221) revealed that there must have been significant depletion of silver before burial. SEM-EDX analysis was carried out on a deep scratch on the surface of K1221 (Figure 9) which appears to have occurred before burial, as it has the same tarnish layer as the undamaged surface. This revealed a similar silver composition to that of the underlying core, i.e. the pre-burial damage had cut through the surface silver depletion. Only a reduction in the copper content was seen on this damaged area (Figure 12). If burial corrosion was the only reason for the depletion in silver (and copper) seen on the undamaged surfaces of other pieces, this scratch would have been expected to show the same depletion in silver as elsewhere on the surface of K1221, but that was not the case.

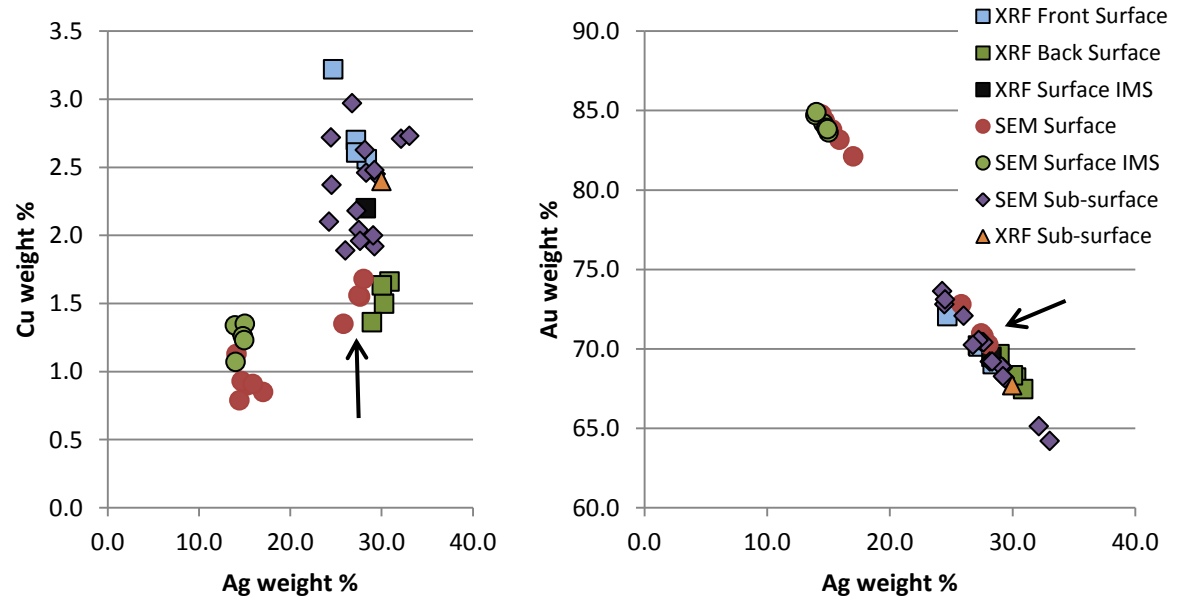

Figure 12. Silver/copper (left) and silver/gold (right) concentration plots of the XRF and SEM-EDX data for K1221. The arrows show the group of surface SEM-EDX analyses representing the scratch.

The two outliers

K133 (Figure 13) was the only object in the pilot study with a base gold composition, (45-50 wt% gold, 45-50 wt% silver and 1.5-3 wt% copper). In this case, the slightly cleaner, burnished, front of the object arguably showed a more enriched surface than the back of the object but further examination by SEM-EDX of the edge of this object revealed that the surface and sub-surface of the back had a very similar composition. That such a base gold alloy showed so little loss of the baser elements, silver and copper, adds to the evidence that the heavy depletion in silver and copper seen in the surface of the other objects may not have occurred entirely naturally through the corroding action of the burial environment. This object was found in approximately the middle of the excavated and surveyed area (Figure 1), so if natural silver depletion was taking place throughout the site, this artefact should have corroded in a similar manner to all other objects.

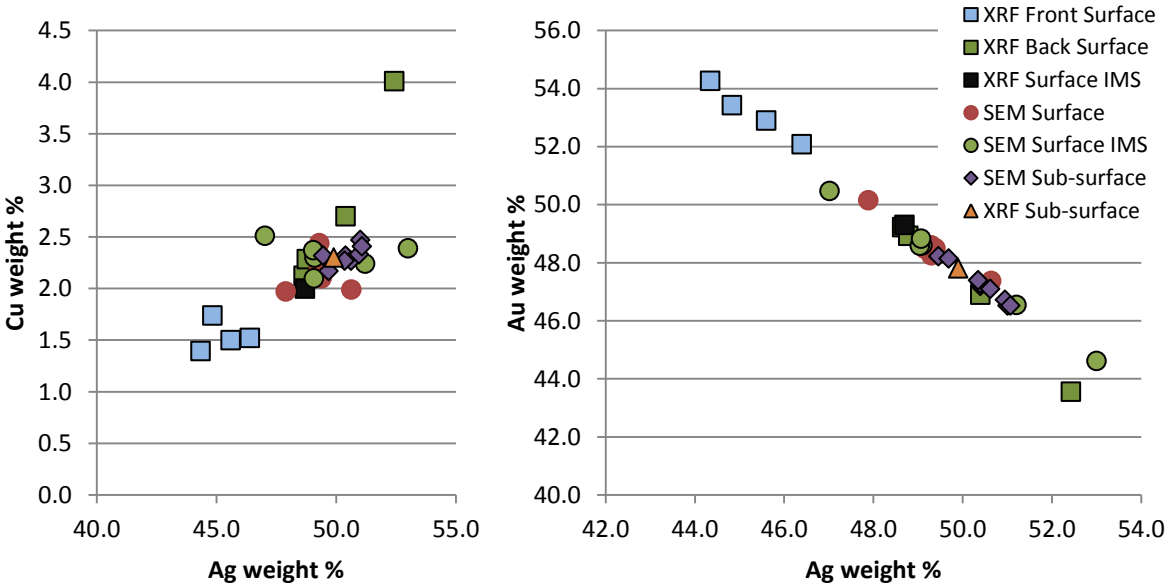

Figure 13. Silver/copper (left) and silver/gold (right) concentration plots of the XRF and SEM-EDX data for K133 showing the difference in composition between the front and back of the piece when analysed by XRF, but the similarities between the surface and subsurface results.

The other outlier K95 had a higher proportion of silver at the surface when compared to the core (Figure 14). As there is no known way of preferentially removing gold, the more noble metal, from the surface of a gold alloy object this may indicate variability in alloy composition within the object itself. This artefact had a large number of platinum group elements (PGE) inclusions and a copper content below 1 wt%, which may suggest the source metal was relatively pure unrefined alluvial gold (Ogden 1977; Raub 1995). The differences seen may thus reflect variation in the composition of the gold-silver alloy source rather than any enrichment or depletion. Another possibility is that the silver was re-deposited from a nearby corroded silver object (Cowell and Hook 2010).

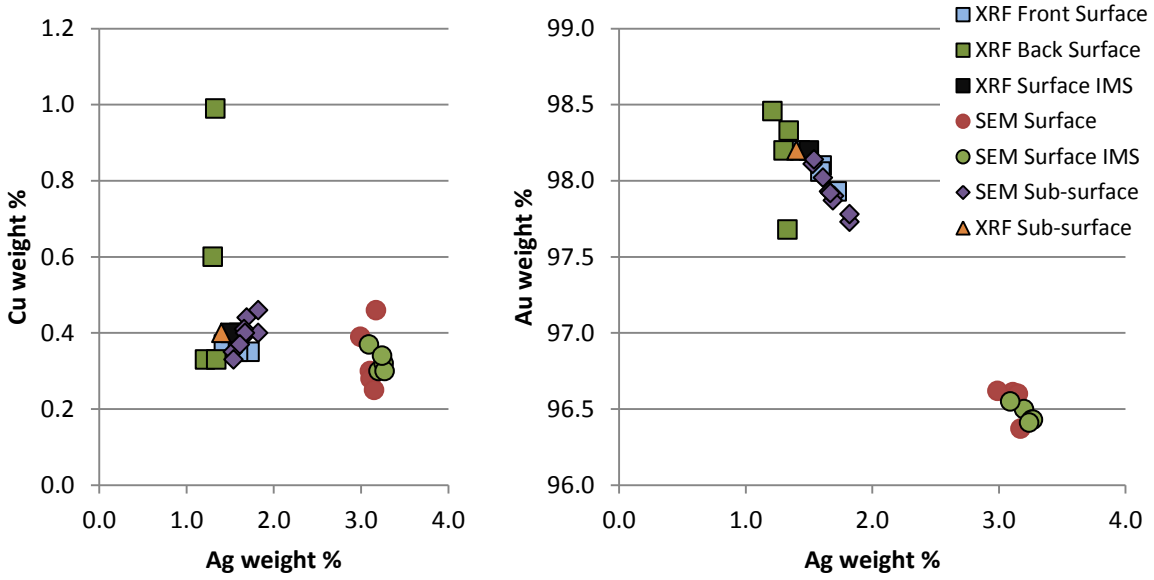

Figure 14. Silver/copper (left) and silver/gold (right) concentration plots of the XRF and SEM-EDX data for K95, showing the higher proportion of silver present at the surface of the object compared to the core.

Surface enrichment in the Staffordshire Hoard

Gold is commonly considered as a chemically very resistant metal, but it is well known that corrosion occurs when it is alloyed with other less noble metals e.g. copper, silver, palladium etc. (Möller 1995). Therefore, depletion in copper from the surface of gold alloy objects can be expected. Copper especially can be removed from gold alloys, in the form of oxides produced by heating the alloy, e.g. by routine annealing, with more than 1% copper removed by pickling during manufacture and further by leaching in the post-depositional environment (Raub 1995). Small quantities of silver can also be lost due to corrosion (Lehrberger and Raub 1995; Voute 1995). Cracks in the surface provide direct access to the metal for a corrosive environment (Lehrberger and Raub 1995).

However the amount of surface depletion in silver documented in many of the pieces, in conjunction with the absence of depletion on the surface of K133 and on the various old scratches analysed, suggests that, in many cases, burial corrosion is not the only cause for the depletion seen in this group of Staffordshire Hoard objects.

Typically any corrosion that occurs during burial (or etching due to chemical cleaning) results in the surface of the object being matted and/or pitted (Forty 1979; Forty 1981). Previous research has shown that bright burnished surfaces may be a sign that the surface is the result of the goldsmith's craft in remedying the dull surface caused by corrosive agents, and thus indicates a as a deliberate treatment carried out by the goldsmith to enhance the surface (Craddock 2000; La Niece 1995). Even so not all matt surfaces have been deliberately surface depleted, as there are archaeological examples where objects have been selectively burnished or deliberately treated afterwards to leave or create an un-reflective surface, though no such examples are reported from Anglo-Saxon gold work (Scott 1983a).

Deliberately induced chemical processing of the surface of artefacts can lead to features similar to corrosion. Depletion gilding is hard to identify from the surface of an object (La Niece 1995; Stern 1995). Silver can be removed in two main ways. The first method is solid-state cementation, the prolonged heating of a gold alloy in a sealed container with salt or alum and an absorbent material, such as clay or brick dust (Craddock 2000; La Niece 1995; Möller 1995).

The second method uses a strong corrosive medium, most likely a combination of ferritic sulphate and salt, to attack the surface of the metal at room temperature for an even longer time (La Niece 1995; Letchman 1973). Copper can also be removed from the surface by oxidisation and subsequent use of weak acids (citric or oxalic) to dissolve the copper oxides (La Niece 1995). This chemically produced enrichment would result in a patina of oxides and salts on the surface of the object and possibly create a pitted surface; burnishing was therefore required to restore a shiny finish, e.g. by rubbing the surface with a smooth tool, usually a hard, polished stone (La Niece 1995; Untracht 1982). Burial in soil will then intensify any intentional process, so apparent corrosion phenomena on artefacts may be both natural and man-made (Möller 1995).

All the above suggests that surface XRF analysis of objects can only provide semi-quantitative data of alloy compositions at best. The marginal zone with heavy depletion in silver and copper can be more than 0.1 mm thick (Lehrberger and Raub 1995), and this pilot study confirms that surface analyses, even with XRF, cannot accurately measure the composition of the original alloy. The incident beam of the SEM-EDX cannot penetrate deep enough below the surface, and the results from the XRF, which can penetrate deeper into the core metal, is heavily influenced by the surface layers. The accurate determination of core compositions of metal objects can only be achieved by either SEM-EDX or XRF sub-surface analysis.

Conclusion

The results from the analysis of sixteen objects have clearly shown that, in many cases, there is significant but not consistent surface enrichment in gold due to the depletion in both copper and silver. The analysis of deep scrapes, probably made when dismantling the swords before burial, confirmed that loss of copper occurred during burial, but showed little loss of silver. However, the comparison between the composition of undamaged surfaces and sub-surfaces suggests that some form of deliberate depletion gilding took place to remove both silver and copper from the surface.

Finding evidence for specific surface treatment during the manufacturing process is difficult, particularly through non-destructive analysis, as it is more commonly identified when cross-sections are taken allowing comparison between the core microstructure of the metal and the treated surface to be studied. At this stage it is difficult to say whether more sophisticated surface treatment was a widespread Anglo-Saxon metalworking practice. This is a small sample of similar artefacts and bias may have been introduced to the results due to the selection of such a specific type of object, as they almost all show similar compositions. Therefore, more work would need to be carried out on a larger range of object types, and particularly objects with multiple components to see whether they vary in composition and surface treatments.

All the above suggests that XRF analysis even with its deeper penetration of the surface of the object can provide only semi-quantitative data of alloy compositions at best. The accurate determination of the core composition of objects can only be achieved by sub-surface analysis using either SEM-EDX and XRF or other invasive or destructive analytical techniques. The unpredictable variability within the surface and sub-surface results means that there is no feasible method to recalculate the sub-surface results using surface XRF or SEM-EDX data (Hall 1961).

Future Work

Surface enrichment in gold correlated to silver and copper depletion has also been observed on a range of gold objects at the British Museum, including a number of Anglo-Saxon objects. The depletion in copper can easily be explained as a post-depositional loss due to corrosion, and a potential surface treatment during manufacturing for which evidence cannot be seen through non-destructive study but the depletion in silver has yet to be explained.

The selection of artefacts for this pilot study may have introduced a degree of bias. The relatively small range of compositions may support this. It is possible that basic objects like hilt plates were being treated when other objects were not. Therefore, more analysis of other types of objects from the Hoard and of objects spanning the Hoard time frame would be required to determine the extent of surface enrichment, especially on more complex objects made from a number of different components.

Previous studies by other researchers have shown that it is possible to understand more about the surface depletion through microstructural analysis especially when combined with chemical analysis (La Niece 1995; Lehrberger and Raub 1995; Voute 1995). The depletion techniques described above have an effect on the surface of the object, and although burnishing removes this evidence, below this burnished surface a porous zone created by the loss in silver and copper can often be seen (Lehrberger and Raub 1995). The silver depletion of the Staffordshire Hoard objects would therefore most likely be better understood through the microscopic examination and analysis of cross-sections. It would be particularly important for any multiple component analysis to determine whether all components were being depleted or whether there was selected depletion of certain components, such as the backing plates for instance. Surface and sub-surface analyses would be necessary to check this, and, wherever possible, more accurate information could be obtained using metallography and SEM-EDX examination on small specimens taken from components.

Scientific examination of gold alloy sheets experimentally produced and subjected to depletion techniques accessible to the Saxon goldsmith may also reveal which methods were being used.

Acknowledgements

I would like to thank Nigel Meeks for all his input while developing the SEM-EDX methodology and for reading and commenting on this report. I would also like to thank Aude Mongiatti, Susan La Niece, Duncan Hook, Philip Fletcher and Catherine Higgitt for reading and commenting on the various drafts of the report.

Eleanor Blakelock Aude Mongiatti Catherine Higgitt

18th December 2013

Appendix 1 - Surface and sub-surface compositional data for individual objects

The pages that follow include the data for all the objects analysed. The tables of results show the average compositions of the surfaces of the front and back analysed by XRF as well as the surfaces and sub-surfaces analysed by SEM-EDX. Also included are the average compositions of surfaces cleaned with IMS and of sub-surfaces analysed by XRF with the 0.2 mm collimator. The graphs on each page plot all the points of analysis, for silver/gold and silver/copper concentrations.

K3

	Wt% Au	Wt% Ag	Wt% Cu
XRF Front	82.2	15.6	2.2
XRF Back	83.5	14.8	1.7
XRF Surface IMS	81.6	16.3	2.1
SEM Surface	90.9	8.1	1.1
SEM Surface IMS	89.7	9.4	0.9
SEM Sub-surface	81.6	15.7	2.6
XRF Sub-surface	82.1	15.5	2.4

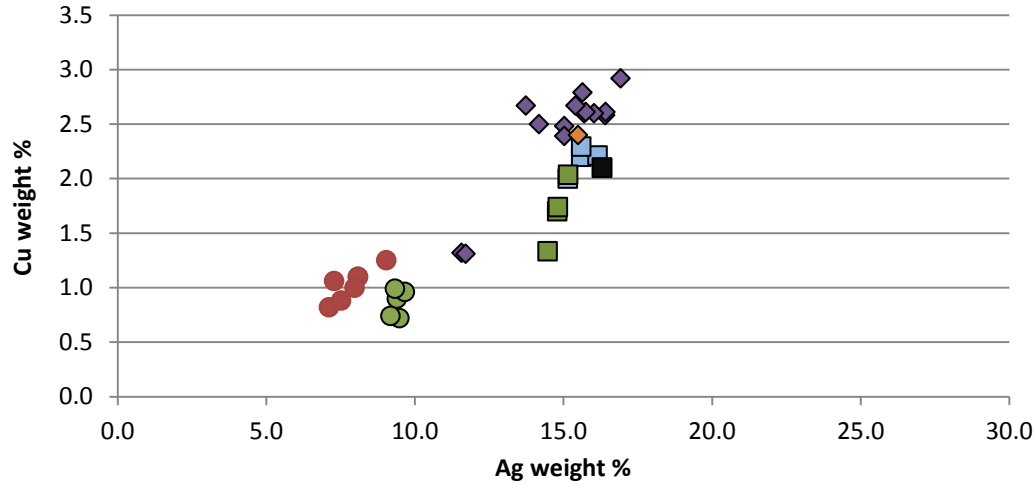

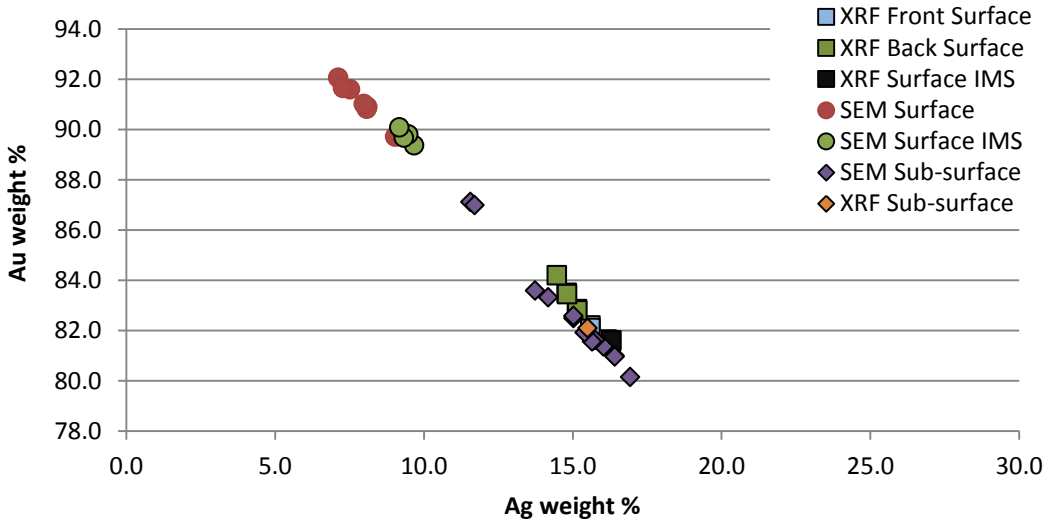

K10

	Wt% Au	Wt% Ag	Wt% Cu
XRF Front	82.4	15.9	1.7
XRF Back	83.6	15.1	1.3
XRF Surface IMS	83.1	15.6	1.3
SEM Surface	88.6	10.4	1.0
SEM Surface IMS	91.5	8.0	0.5
SEM Sub-surface	82.8	14.9	2.3
XRF Sub-surface	82.0	15.8	2.2

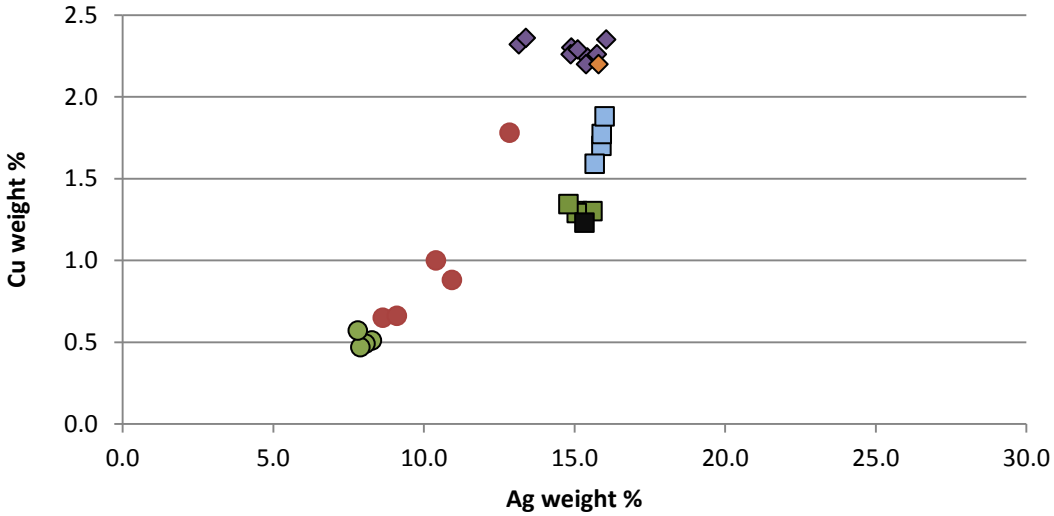

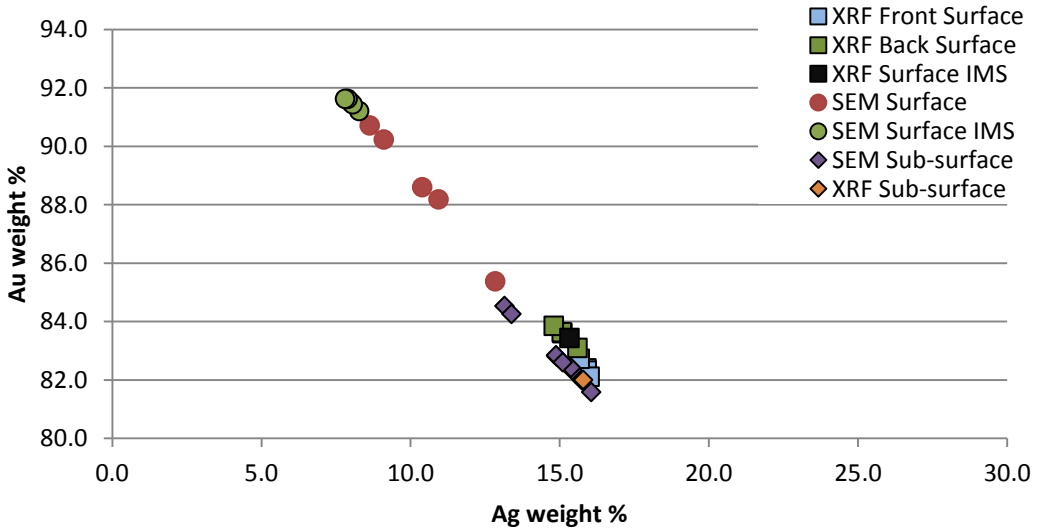

K12

	Wt% Au	Wt% Ag	Wt% Cu
XRF Front	78.0	19.5	2.5
XRF Back	77.4	17.6	5.0
XRF Surface IMS	78.7	19.2	2.1
SEM Surface	86.5	12.4	1.2
SEM Surface IMS	85.8	13.2	1.0
SEM Sub-surface	77.5	20.2	2.3
XRF Sub-surface	78.5	19.3	2.1

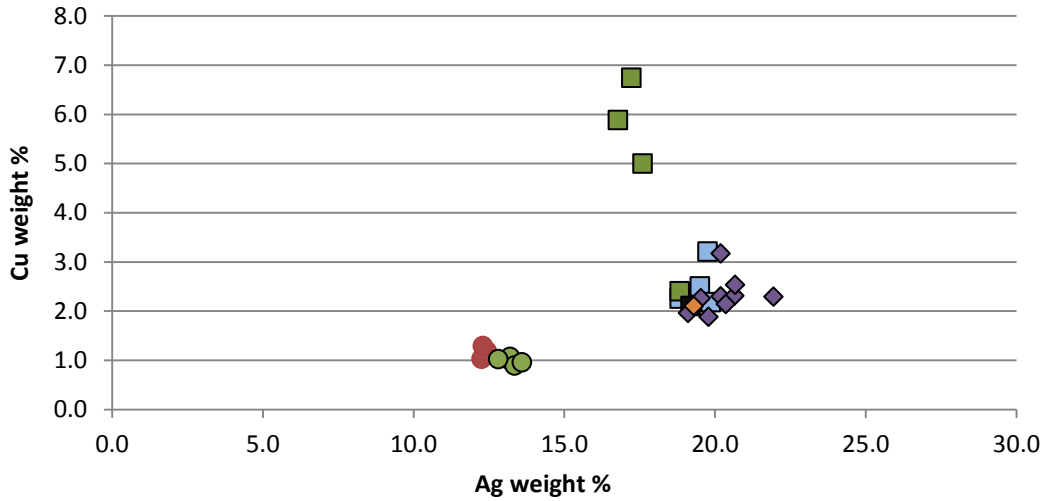

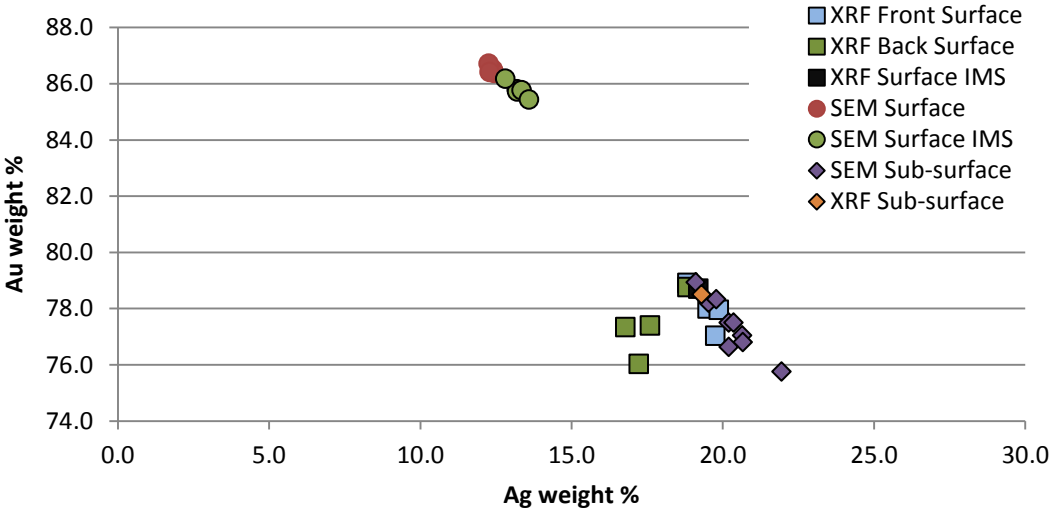

K79

	Wt% Au	Wt% Ag	Wt% Cu
XRF Front	75.8	22.9	1.3
XRF Back	76.3	22.6	1.1
XRF Surface IMS	76.3	22.6	1.1
SEM Surface	70.0	29.2	0.8
SEM Surface IMS	71.9	26.9	1.1
SEM Sub-surface	72.0	26.4	1.7
XRF Sub-surface	75.1	23.4	1.5

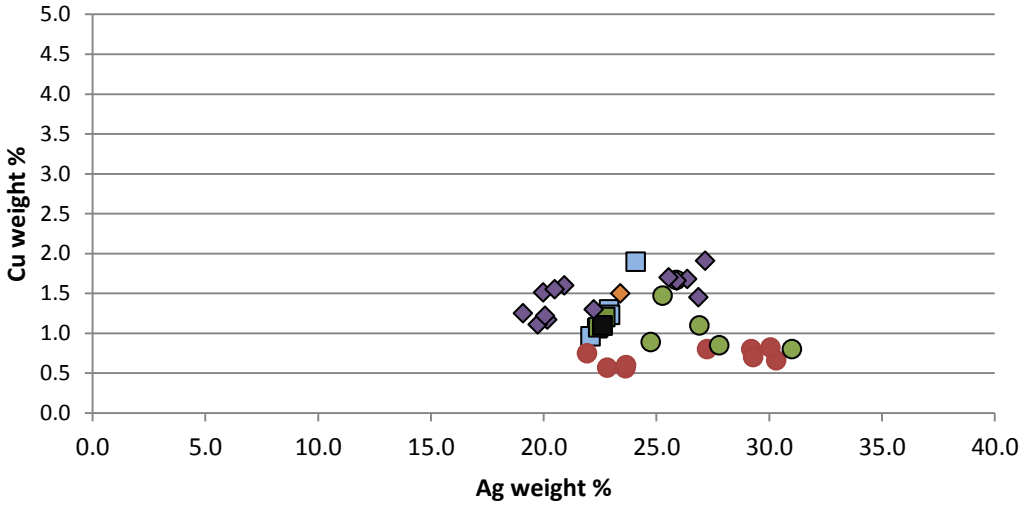

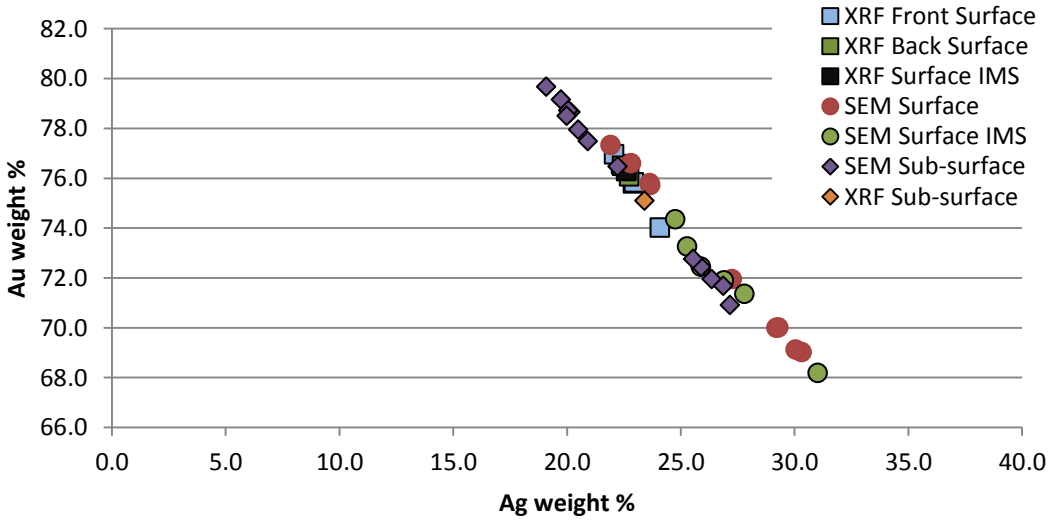

K95

	Wt% Au	Wt% Ag	Wt% Cu
XRF Front	98.1	1.6	0.4
XRF Back	98.2	1.3	0.6
XRF Surface IMS	98.2	1.5	0.4
SEM Surface	96.6	3.1	0.3
SEM Surface IMS	96.5	3.2	0.3
SEM Sub-surface	97.9	1.7	0.4
XRF Sub-surface	98.2	1.4	0.4

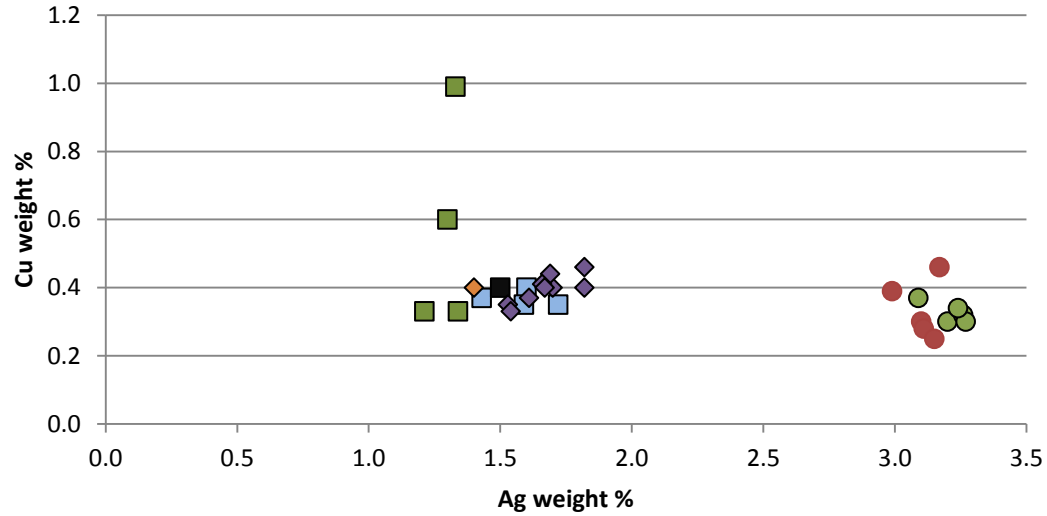

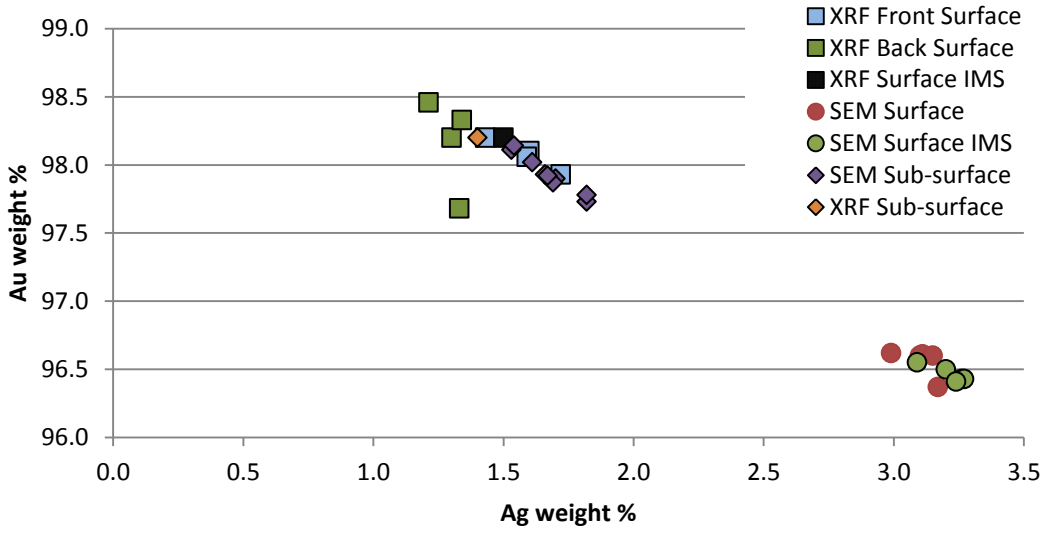

K133

	Wt% Au	Wt% Ag	Wt% Cu
XRF Front	52.9	45.6	1.5
XRF Back	46.9	50.4	2.7
XRF Surface IMS	49.3	48.7	2.0
SEM Surface	48.6	49.3	2.2
SEM Surface IMS	48.6	49.1	2.3
SEM Sub-surface	47.2	50.4	2.3
XRF Sub-surface	47.8	49.9	2.3

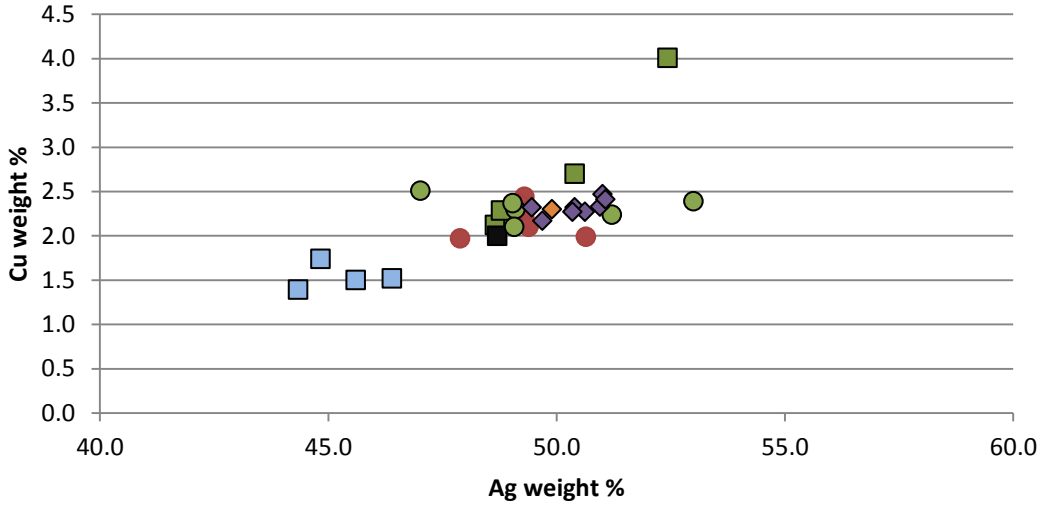

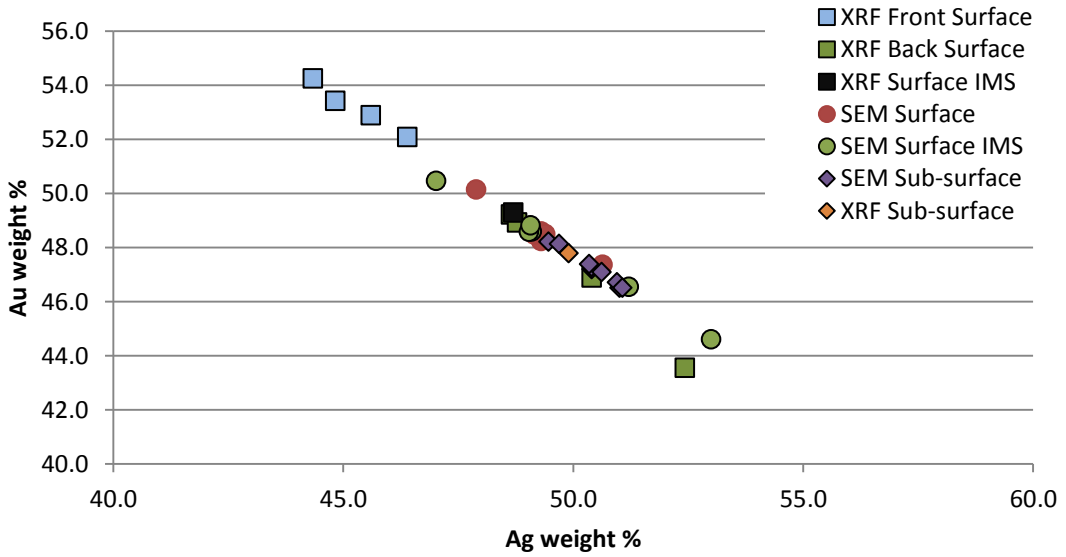

K1048

	Wt% Au	Wt% Ag	Wt% Cu
XRF Front	78.2	19.5	2.3
XRF Back	78.7	19.7	1.7
XRF Surface IMS	79.3	18.9	1.8
SEM Surface	83.2	15.2	1.6
SEM Surface IMS	83.4	15.0	1.6
SEM Sub-surface	80.0	17.9	2.1
XRF Sub-surface	79.2	19.0	1.9

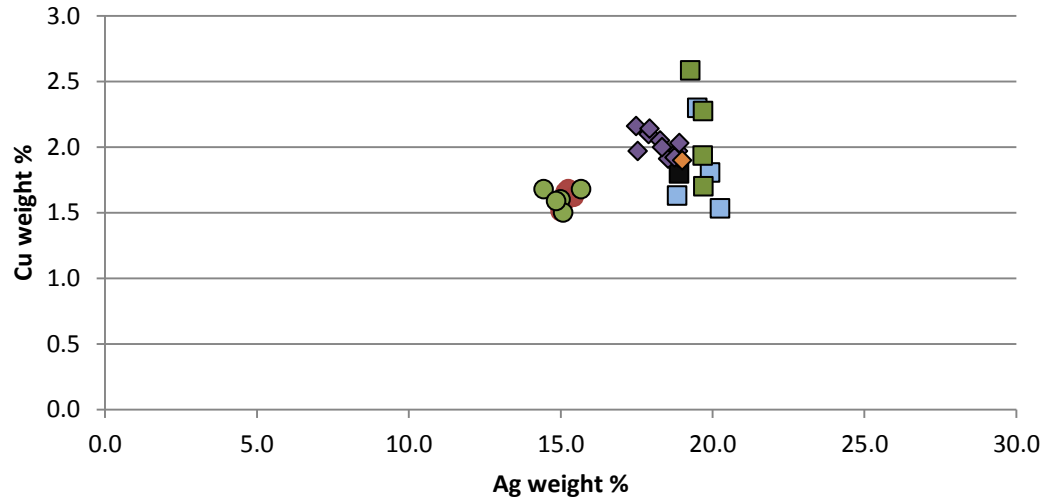

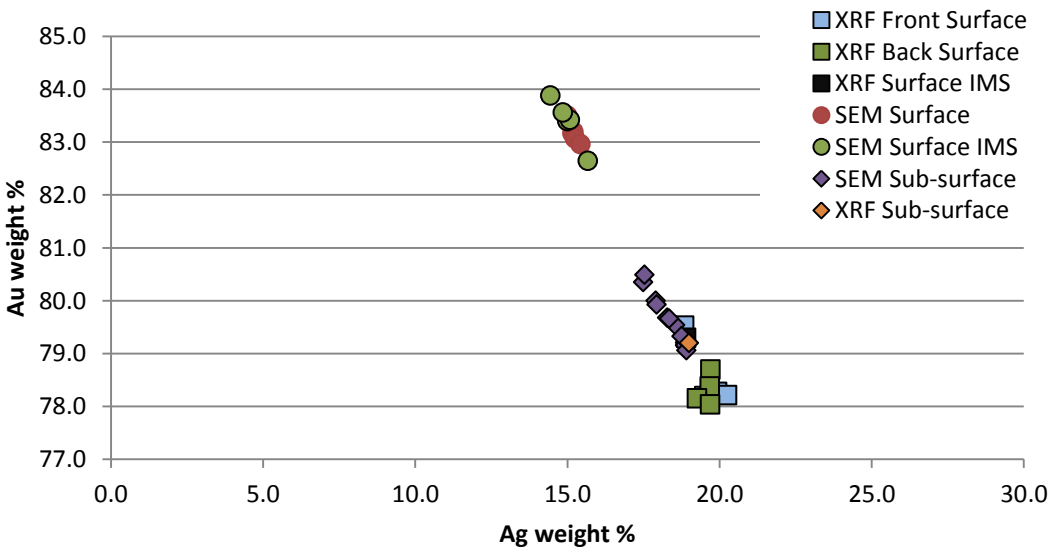

K1072

	Wt% Au	Wt% Ag	Wt% Cu
XRF Front	81.4	17.1	1.4
XRF Back	80.8	17.9	1.3
XRF Surface IMS	80.9	17.8	1.4
SEM Surface	81.7	17.5	0.8
SEM Surface IMS	81.8	17.4	0.8
SEM Sub-surface	78.6	19.7	1.7
XRF Sub-surface	80.1	18.4	1.5

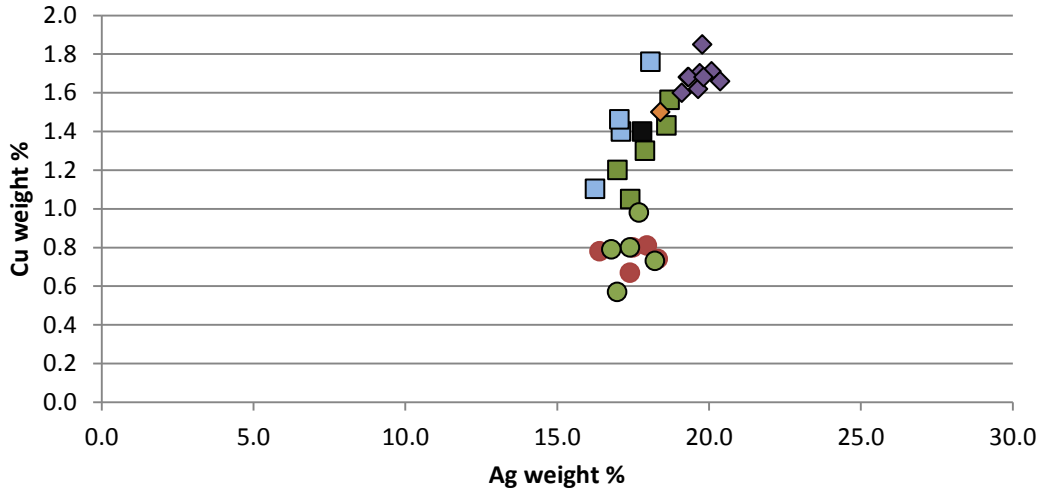

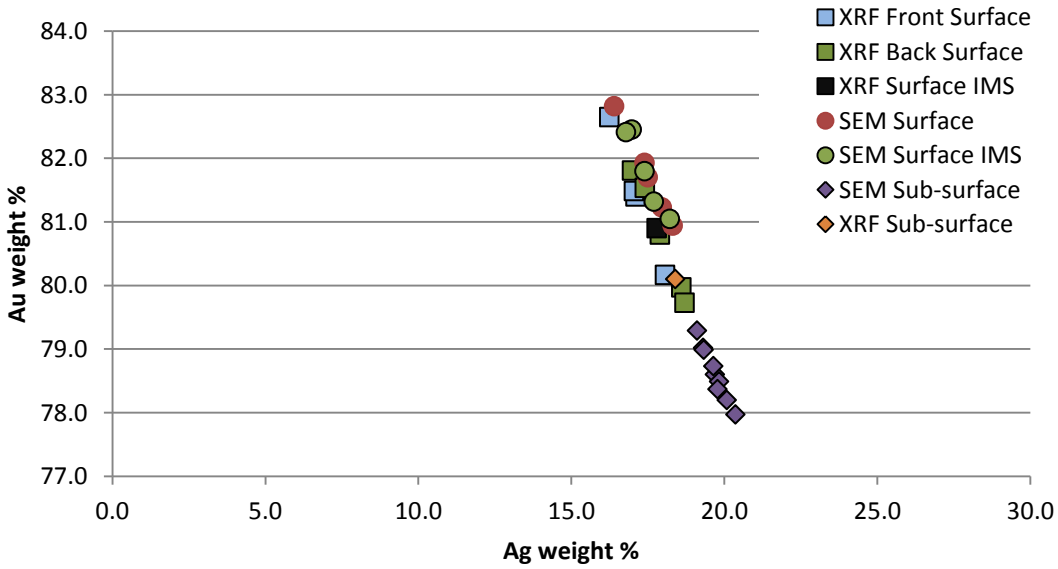

K1136

	Wt% Au	Wt% Ag	Wt% Cu
XRF Front	79.4	18.6	1.9
XRF Back	76.1	22.6	1.3
XRF Surface IMS	79.1	18.7	2.3
SEM Surface	77.2	21.6	1.2
SEM Surface IMS	77.1	21.9	1.0
SEM Sub-surface	76.9	20.6	2.6
XRF Sub-surface	78.3	19.1	2.6

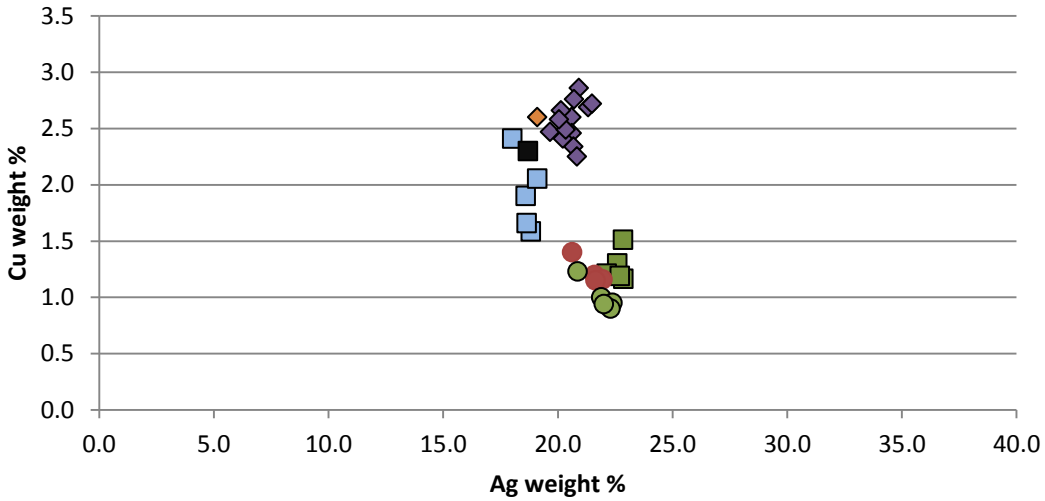

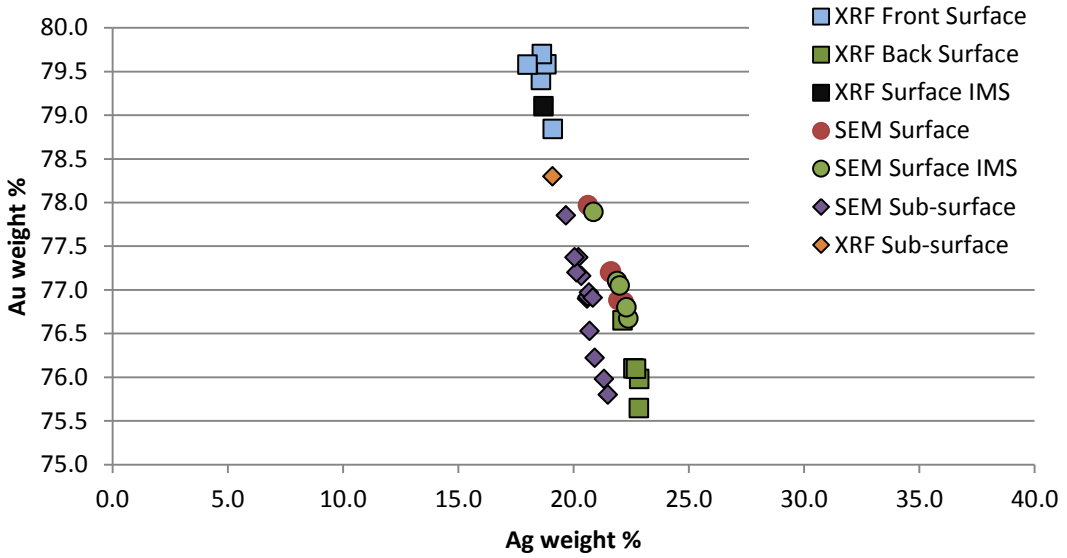

K1137

	Wt% Au	Wt% Ag	Wt% Cu
XRF Front	74.5	23.4	2.1
XRF Back	72.7	25.5	1.8
XRF Surface IMS	72.7	25.4	1.9
SEM Surface	75.2	23.7	1.1
SEM Surface IMS	74.8	24.0	1.2
SEM Sub-surface	71.8	26.0	2.0
XRF Sub-surface	72.6	25.4	2.0

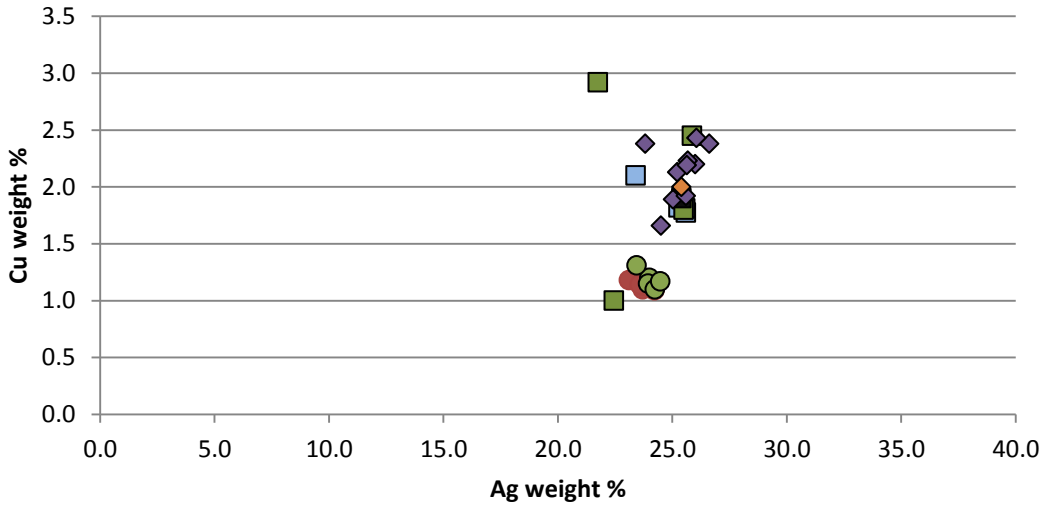

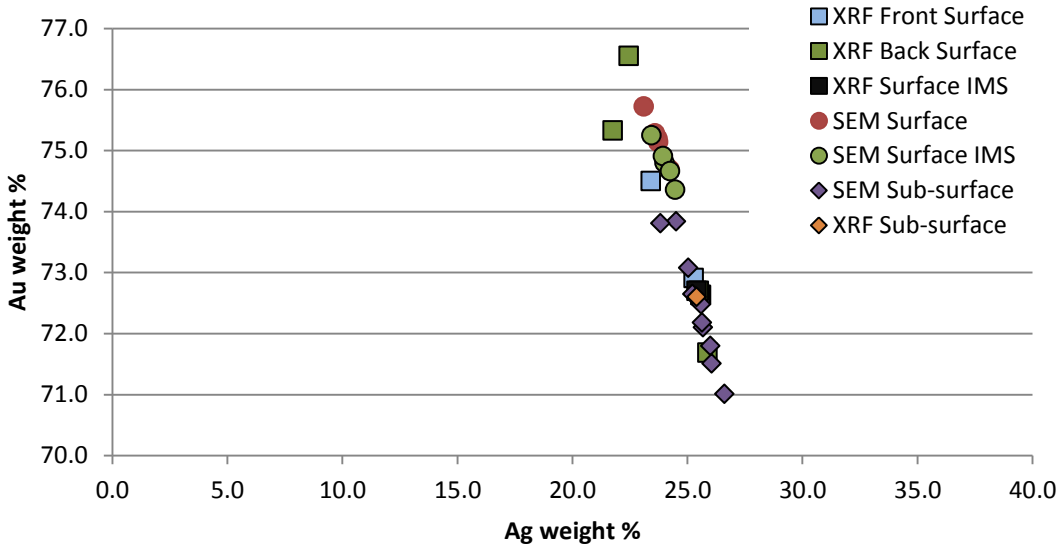

K1143

	Wt% Au	Wt% Ag	Wt% Cu
XRF Front	84.6	14.1	1.3
XRF Back	82.2	15.9	1.9
XRF Surface IMS	83.1	15.3	1.5
SEM Surface	85.5	13.5	1.0
SEM Surface IMS	85.1	13.7	1.2
SEM Sub-surface	83.3	14.6	2.1
XRF Sub-surface	82.3	16.0	1.7

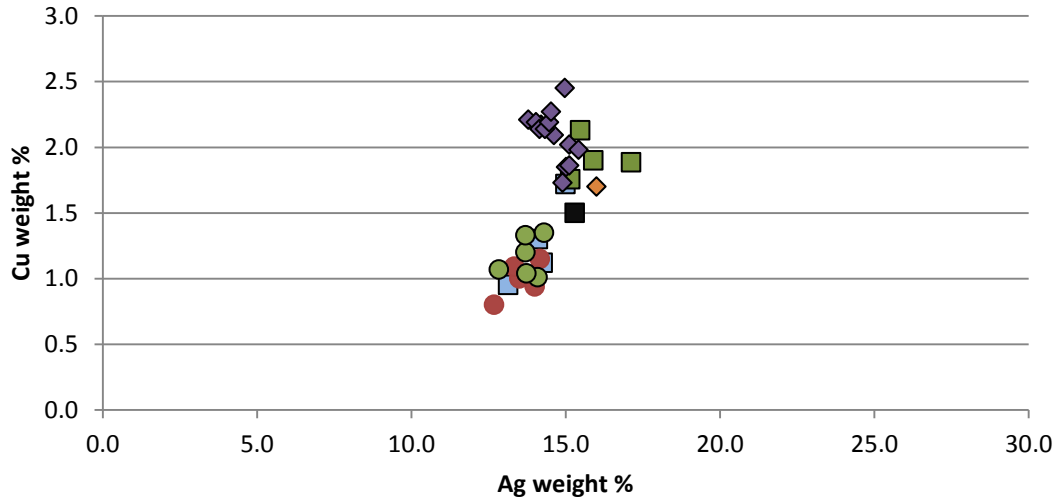

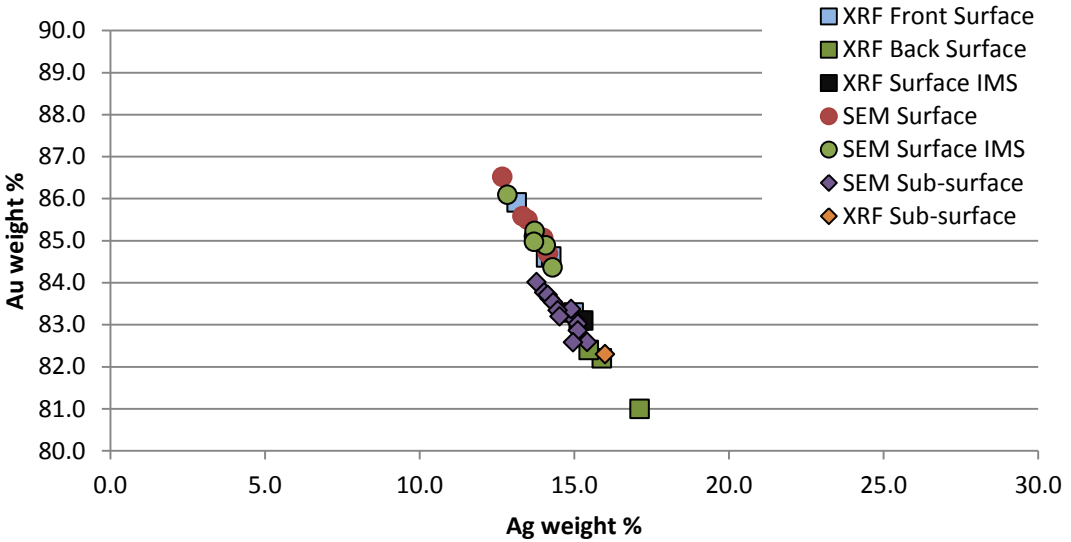

K1150

	Wt% Au	Wt% Ag	Wt% Cu
XRF Front	82.9	15.5	1.6
XRF Back	79.7	15.1	5.2
XRF Surface IMS	83.6	14.9	1.4
SEM Surface	92.8	6.3	0.9
SEM Surface IMS	92.4	6.7	1.0
SEM Sub-surface	82.2	15.9	1.9
XRF Sub-surface	83.9	14.4	1.7

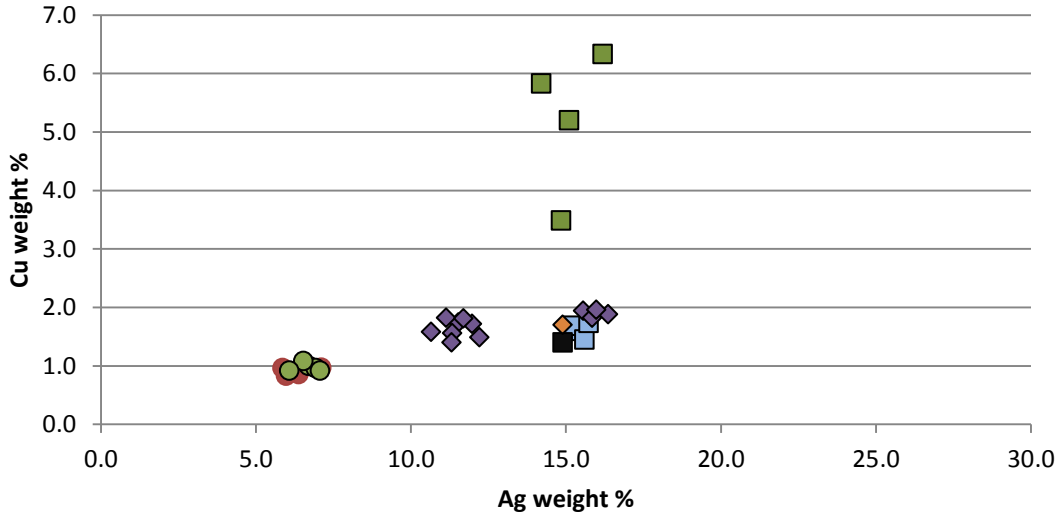

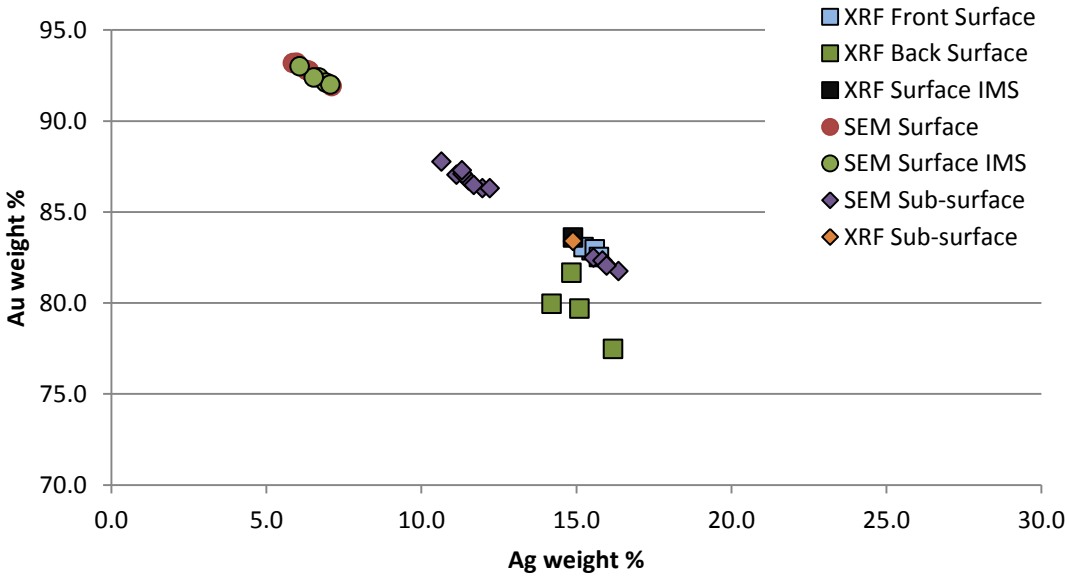

K1163

	Wt% Au	Wt% Ag	Wt% Cu
XRF Front	74.0	24.0	2.0
XRF Back	74.2	24.3	1.5
XRF Surface IMS	74.9	23.2	1.9
SEM Surface	81.0	17.7	1.3
SEM Surface IMS	80.9	17.1	1.9
SEM Sub-surface	75.3	22.7	1.9
XRF Sub-surface	73.4	23.9	2.7

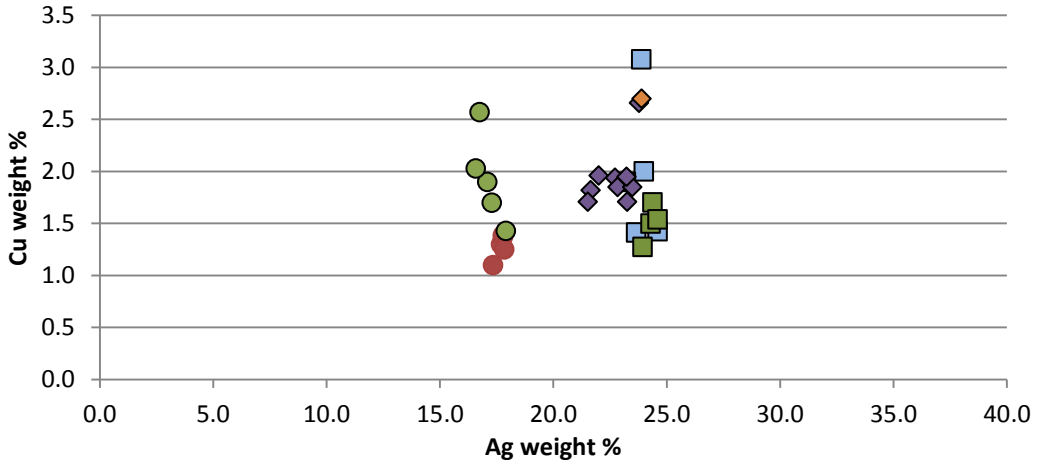

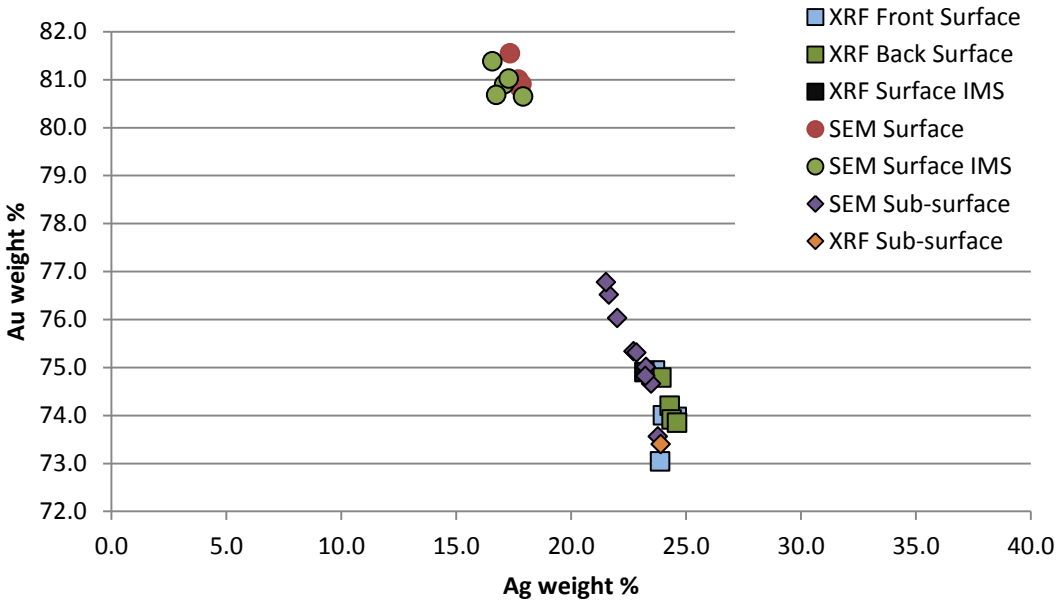

K1221

	Wt% Au	Wt% Ag	Wt% Cu
XRF Front	70.2	27.2	2.7
XRF Back	68.2	30.3	1.5
XRF Surface IMS	69.5	28.3	2.2
SEM Surface	83.8	15.3	0.9
SEM Surface IMS	84.2	14.6	1.3
SEM Sub-surface	69.2	28.2	2.6
XRF Sub-surface	67.7	30.0	2.4

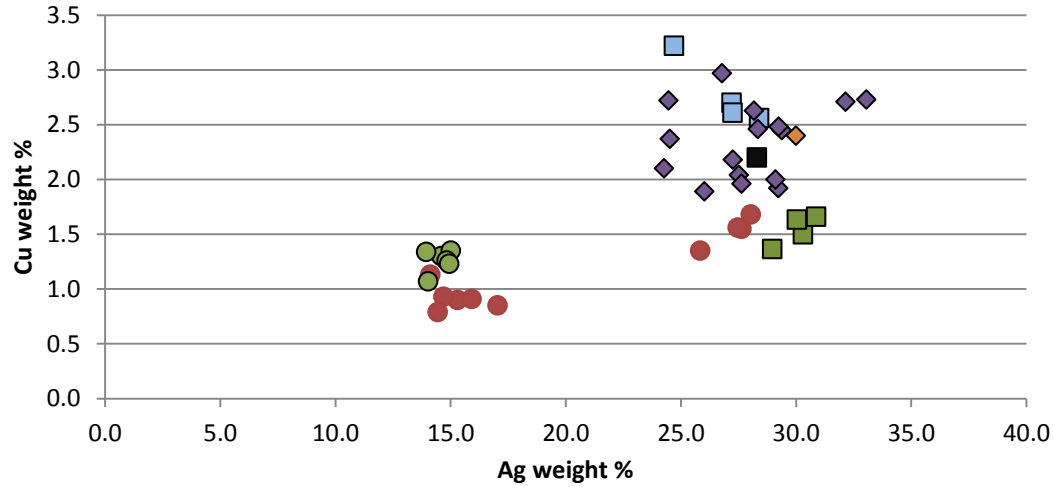

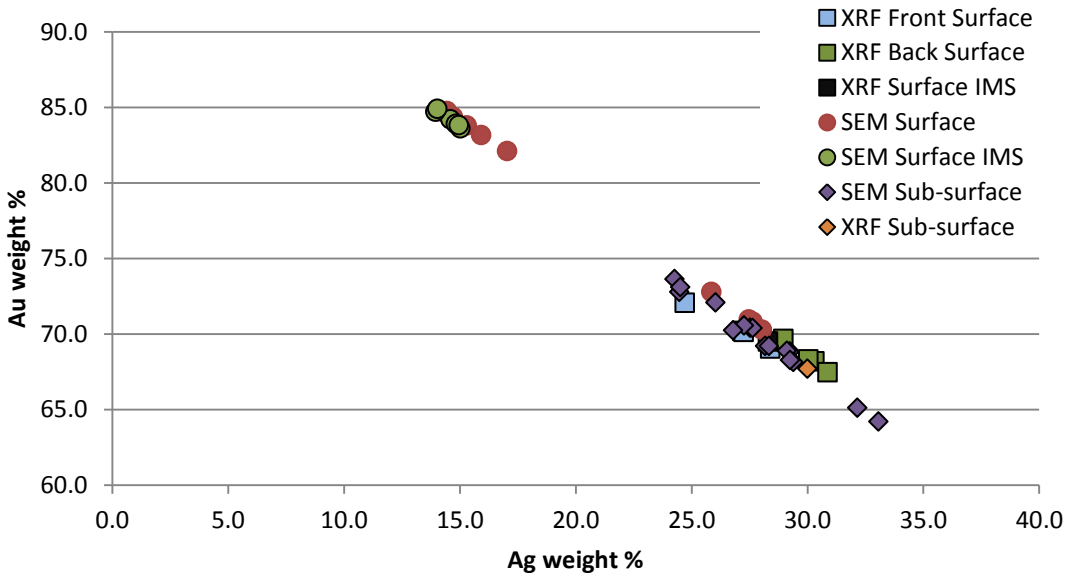

K1234

	Wt% Au	Wt% Ag	Wt% Cu
XRF Front	79.8	18.4	1.8
XRF Back	79.3	19.2	1.5
XRF Surface IMS	79.0	19.3	1.6
SEM Surface	87.6	11.5	0.9
SEM Surface IMS	88.4	10.7	0.9
SEM Sub-surface	79.8	18.1	2.1
XRF Sub-surface	79.1	19.4	1.6

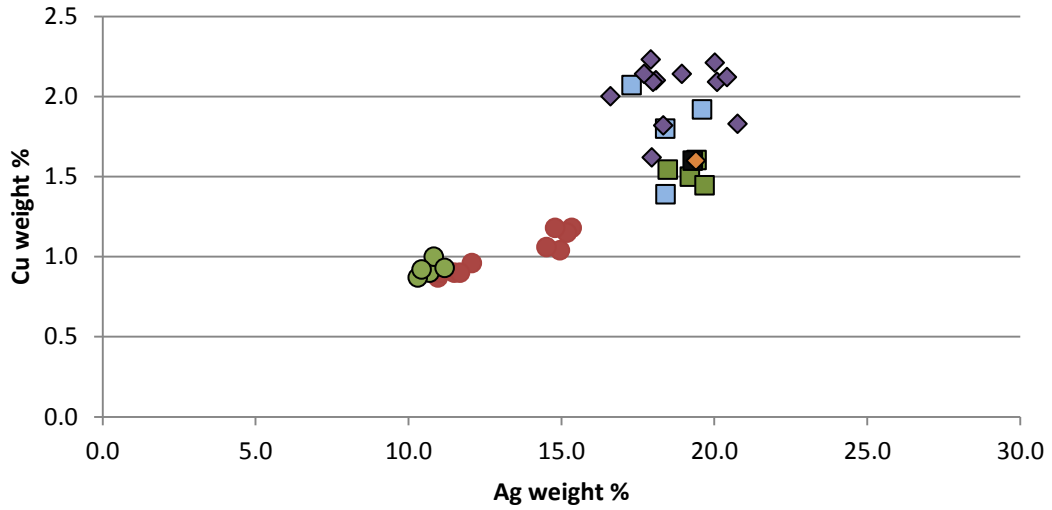

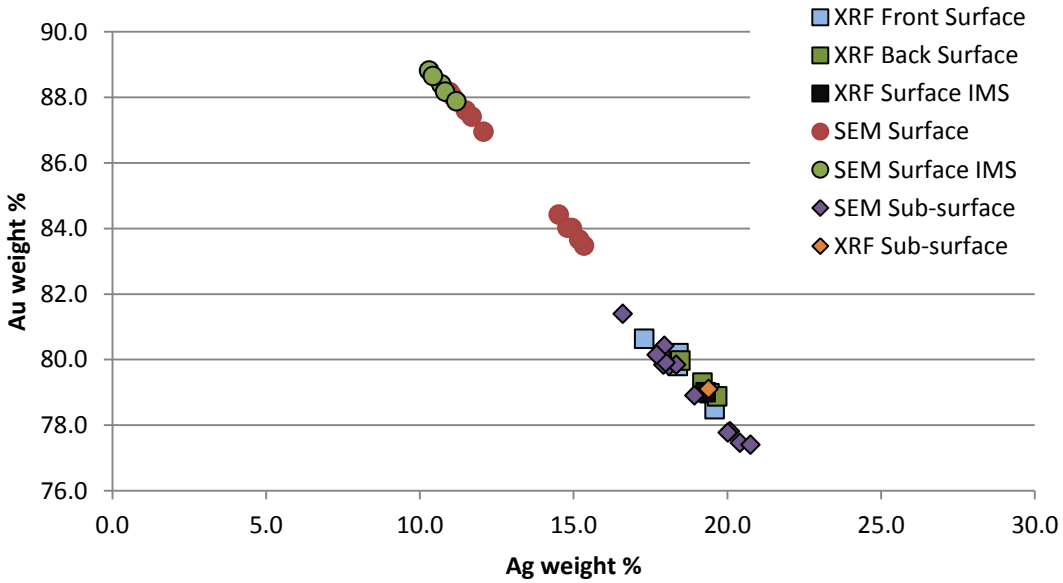

K1272

	Wt% Au	Wt% Ag	Wt% Cu
XRF Front	82.9	15.3	1.9
XRF Back	82.6	15.5	1.9
XRF Surface IMS	80.1	16.4	3.5
SEM Surface	84.0	13.5	2.6
SEM Surface IMS	85.1	12.8	2.1
SEM Sub-surface	80.7	15.1	4.1
XRF Sub-surface	80.8	16.2	2.9

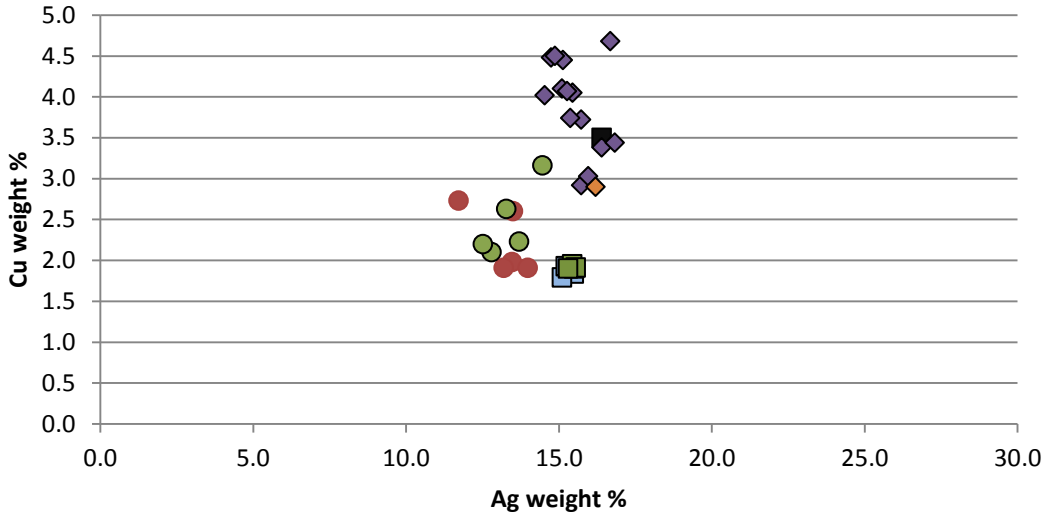

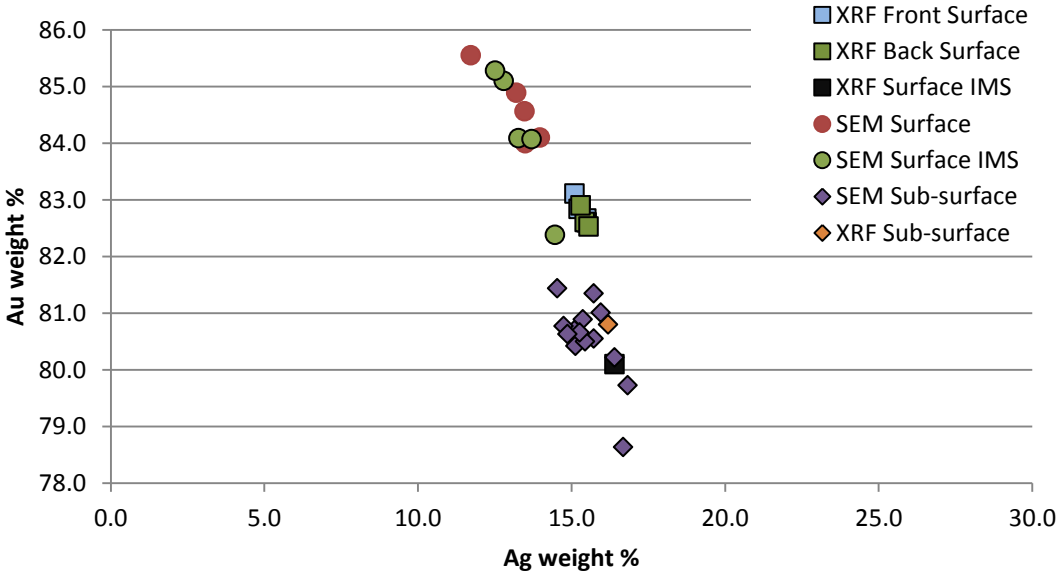

Appendix 2 – Introduction to XRF and SEM Techniques

This section aims to provide a basic introduction to both XRF and SEM-EDX techniques.

XRF

In XRF analysis X-rays of relatively high energy are used to bombard the material (incident X-rays); this causes electrons to be ejected from the atoms making up the material. This in turn causes an electron from an outer shell to fall into the space in the inner shell, left by the ejected electron, which releases the excess energy in the form of fluorescent x-ray (Figure 15). This energy called X-ray fluorescence can be detected and measured to determine the atom/element present, and the intensity of the energy is proportional to the amount of an element present therefore quantification is possible (Cowell 1998).

Signals of different energy are produced depending on which atomic shells electrons move down from e.g. from the M shell to the K shell or from the L shell to the K shell. Thus spectra for any single element will have multiple peaks, for example Kα, Kβ, Lα and Lβ peaks (Verma 2007), corresponding to these different signals.

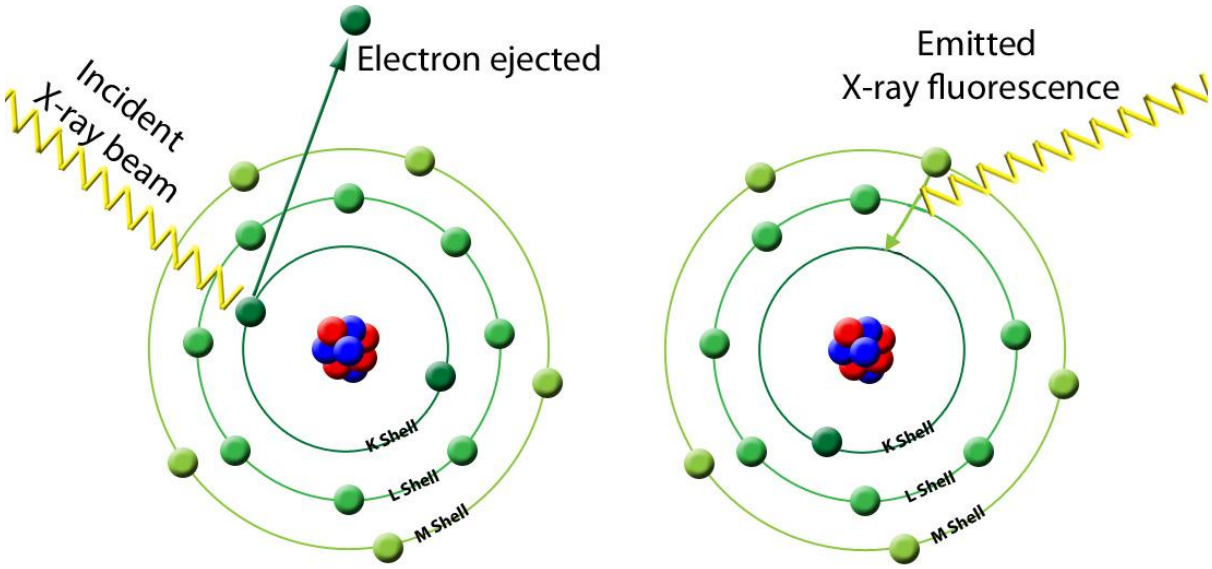

Figure 15. Basic principle of XRF based on descriptions by Cowell (1998) and Verma (2007). SEM-EDX analysis is similar but instead of an X-ray beam, incident high energy electron beams are used to eject atomic electrons.

XRF is one of the most common methods for precious metal analysis, due to its non-destructive nature (Tate 1986). Quoted acceptable errors for the accuracy are ±1-2% relative for flat standards and the precision is very high, ±0.5% relative, decreasing nearer the detection limit to ±25% relative (Cowell 1998). As mentioned in the main text, XRF is a quantitative method if the sample is homogeneous and if the surface is flat, clean and free of corrosion layers. Archaeological objects seldom match these pre-requisites so the results are therefore only qualitative or semi-quantitative (Stern 1995).

The signal received by the XRF (and also the SEM-EDX) detector does not come solely from the area on the surface onto which the excitation beam is focused. X-rays are generated from a volume beneath the surface, the size and depth of which is determined by the atomic density of the material(s) being analysed (Figure 2, Goldstein *et al.* 2003) and the intensity of

the excitation beam. The signal received depends on both the penetration of the beam beneath the surface and also the ability of the signal to return through the sample matrix (Goldstein *et al.* 2003). This means that the actual depth to which gold in a gold alloy can be measured is less than the depth the excitation beam penetrates.

The BM XRF instrument applies the fundamental parameter calculation for quantification.[6] The fundamental parameter methods are based on equations devised by Sherman and consider both primary and secondary fluorescence. Secondary fluorescence is caused when the photons given off when an electron is emitted from the first atom, interact with another atom giving off another photon. The fundamental parameter methods have several advantages. First of all, these methods can be applied in analysis of thick samples, thin films and multilayers. Another advantage of fundamental parameter methods is the possibility of using any standard specimen for calibration: pure-element standard, one standard similar to unknown sample, series of standards similar to unknown sample, etc. Even so the fundamental parameter methods have some limitations, they do not usually consider all physical processes in the sample such as: tertiary fluorescence, scatter of both the primary and fluorescence radiation and photoelectrons used to detect lighter elements. Moreover, the accuracy of fundamental parameters methods strongly depends on uncertainty of atomic parameters (how strongly the matrix absorbs or scatters the X-rays, fluorescent yield, etc.), measurement geometry and spectral distribution of X-ray tube. Nevertheless, the use of standards similar to the unknown will compensate these effects and will lead to more accurate results.

SEM-EDX

There are two parts to the scanning electron microscope with an energy dispersive X-ray detector (SEM-EDX). The first is the Scanning Electron Microscope; this is a type of microscope that produces images of a sample or object by scanning it with a focused beam of electrons, thus allowing for very high magnification (10-10,000x magnification). The electrons interact with electrons in the sample, producing various signals that can be detected and that contain information about the sample's surface topography and composition (Goldstein et al. 2003). When combined with an energy dispersive X-ray (EDX) detector the system can be used to determine the composition of the sample or object. This uses the electron beam to excite and eject electrons from the atom, and results in a fluorescent x-ray (Goldstein et al. 2003; Northover 1998).

Hence the SEM-EDX is a close cousin to the XRF technique based on the production and quantification of X-ray spectra (Northover 1998). The EDX system has a higher limit of detection at 0.1% and the accuracy is ±1% for major and ±10% for minor elements below 1% (Northover 1998). The major disadvantage of this technique is the penetration depth which is even shallower than XRF. The electron beam cannot penetrate much below 5 µm (0.005 mm (Goldstein et al. 2003). For true quantitative analysis flat and polished surfaces are required (Northover 1998).

Variations in apparent composition are due to the fundamental physics of X-ray generation within the surface of the object. In SEM-EDX as well as the corrections introduced by the Oxford INCA software, the term 'ZAF' is used to control and rectify/accommodate for the effects of the mass (or atomic number Z), absorption (A) and any secondary fluorescence (F) as the characteristic fluorescent X-ray makes its way through the sample matrix to the

[6] This software uses fundamental parameters with standards, an approach which was found to be the best for quantitative analysis of copper alloys in a recent study of results produced by laboratories (Heginbotham *et al.* 2011).

instrument detector (Goldstein *et al.* 2003). The instrument software applies this 'ZAF' data along with the fixed sample-detector geometry in a mathematical correction to the peak data from the spectra to give the correct composition. Any changes in sample geometry (curvature or take-off angle) from the fixed sample-detector geometry inherent to the ZAF correction will result in different absorption and fluorescence characteristics in the sample that do not match the pre-determined ZAF correction, yielding incorrect compositional values. Thus differences in the take-off angle, i.e. between the sample and the fluorescent X-ray, will therefore affect the apparent composition (Figure 16). For example, as the angle increases, the fluorescence X-ray travels through a small proportion of the sample matrix, but at a shallower take-off angle these X-rays travel through more matrix and are therefore absorbed to a greater degree.

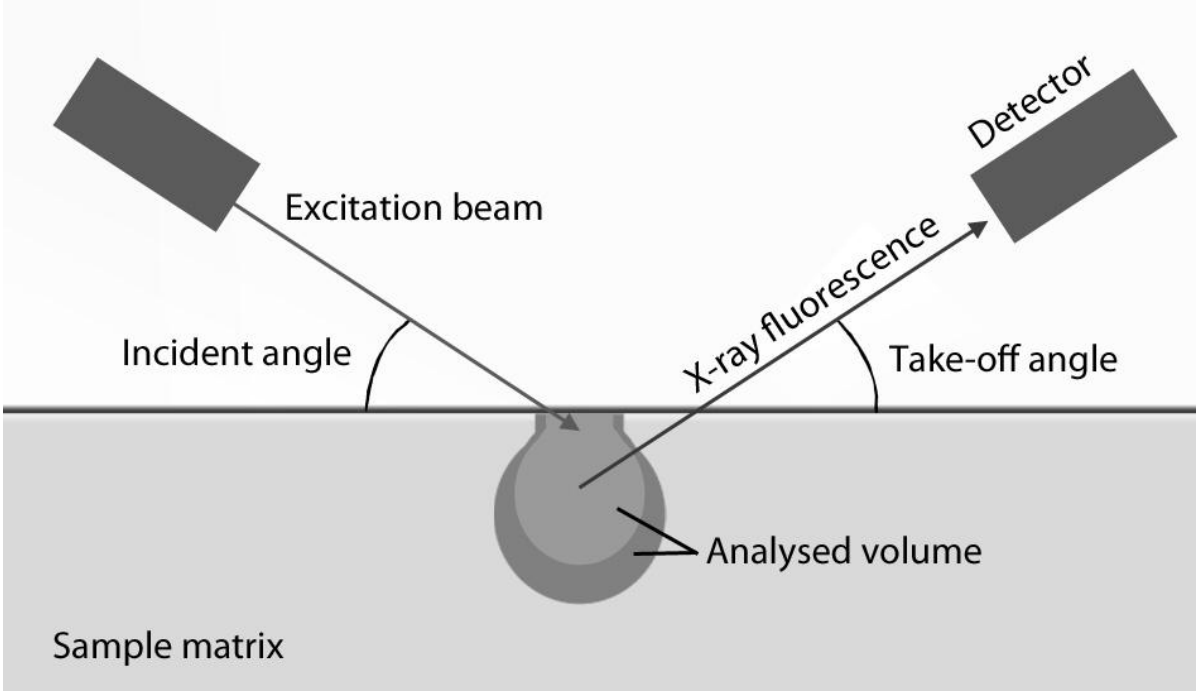

Figure 16. Diagram showing the relationship between the excitation beam and the fluorescent x-ray produced based on descriptions by Verma (2007) and (Goldstein *et al.* 2003). The diagram also shows the area that is being excited beneath the surface of the sample, the size and depth of which is determined by the atomic number of the material (dark grey shows the penetration volume of the beam for low atomic number while the lighter grey volume shows the penetration volume of the beam for high atomic number) and the intensity of the excitation beam.

Appendix 3 – XRF and SEM-EDX analysis of selected standards

A range of gold alloy standards made in-house at the British Museum (referred to as 'SB' standards) were analysed by both XRF and SEM-EDX. This allows for easier comparison between the data gathered by the two instruments. The MAC standards comprise of three certified alloy standards made externally by Micro-Analysis Consultants Ltd for the Staffordshire Hoard project. Three sets were produced, two for the owning institutions Birmingham Museum Trust (BMT) and the Stoke Pottery Museum and Art Gallery (PMAG), and one for the British Museum (BM). These were also examined by both techniques, and are referred to as MAC1, 2 and 3 in this document and related reports. The list of standards used and their compositions are in table 4 below.

	Wt% Au	Wt% Ag	Wt% Cu	Wt% Sn
SB8A	71.0	24.1	4.9	
SB11	85.4	9.6	5.0	
SB12	90.0	5.0	5.0	
SB17	65.9	28.2	5.9	
SB18	63.4	27.2	9.4	
SB39	50.0	30.0	20.0	
MAC1	93.9	4.6	1.0	0.5
MAC2	74.7	19.2	5.1	1.0
MAC3	59.4	29.8	9.1	2.0

Table 4. List of standards and their accepted or certified compositions. Note: no tin is present in the SB standards.

XRF Analysis of the Standards

When quantifying the data from a spectrum, the BM in-house software uses a maximum of four accepted or certified alloy compositions to standardise against, producing compositional data in weight percentage. As with all analytical methods it is important that the range of the standards covers that of the unknown samples to reduce errors due to extrapolation, therefore standards with similar gold alloy compositions are used to create a method (Cowell 1977).

A new standardisation method was created for this research pilot using the standards MAC 1 to 3; this will be referred to as the Staffordshire Hoard Method. The composition of the gold alloys used as standards in this method covered the majority of the range of compositions likely to occur in the Staffordshire Hoard assemblage. However two additional standardisation methods were set up for high-gold and mid- to base-gold alloys. These two additional methods used a combination of two Staffordshire Hoard MAC standards and two SB standards (Table 5).

Methods				
BM High Gold Method	**BM Base Gold Method**	**Staffordshire Hoard Method**	**Staffordshire Hoard High Gold Method**	**Staffordshire Hoard Mid Gold Method**
SB12	SB54[7]	MAC1	MAC1	MAC2
SB39	SB55[5]	MAC2	MAC2	MAC3
SB8A		MAC3	SB11	SB39
			SB8A	SB8A

Table 5. XRF standardisation methods, two existing BM ones and three newly created ones for the Staffordshire Hoard pilot study and the standards used for each.

The average compositional data obtained for a number of standards using the three new Staffordshire Hoard standardisation methods are compared in Table 8 with the results obtained using the existing BM methods. These results show that the Staffordshire Hoard High-Gold method is more accurate, and therefore closer to the certified composition, for high gold alloys in the range 70-100 wt% gold, 0-25 wt% silver and up to 5 wt% copper than the BM High Gold and base Gold methods. The newly created Mid-Gold method is more suited for gold alloys between 50-70 wt% gold, 20-30 wt% silver and 5-20 wt% copper. The Staffordshire Hoard method created using only the MAC standards unsurprisingly gave the most accurate results when analysing the MAC standards, even so the other standardisation methods produced equally reliable data when compared to the accepted standard compositions. Unless otherwise stated, the XRF data included in this report will be quoted using the Staffordshire Hoard High Gold method.

SB8A was used as the standard regularly analysed by XRF during the pilot study (Table 6).

	Wt% Au	**Wt% Ag**	**Wt% Cu**
Accepted Value	**71.0**	**24.1**	**4.9**
08/02/2013	71.0	23.9	5.1
07/02/2013	70.9	24.0	5.1
17/10/2012	71.3	23.7	5.0
15/11/2012	71.3	23.6	5.1
12/02/2013	71.2	23.7	5.1
14/02/2013	70.8	24.1	5.1
08/02/2013	71.0	23.9	5.1
15/02/2013	71.3	23.6	5.1
19/02/2013	71.2	23.7	5.1

Table 6. Normalised results from the analysis of SB8A by XRF, each time it was used during this pilot study.

SEM Standards & Standardisation

The INCA software of the EDX microanalysis system was standardised for gold, silver and copper using the British Museum SB18 standard, which is very close in composition of the majority of the objects selected for the Staffordshire Hoard gold enrichment pilot study. Six SB standards and three MAC standards were analysed at x100 magnification. For each standard, ten analyses were carried out in the same area (*c.* 1200 µm x 1000 µm in size) and the average of the results calculated (Table 9).

Since MAC2 also has a composition close to the majority of objects to be examined within the surface enrichment pilot project, it was also tested for use in the standardisation of gold,

[7] SB54 has 48 wt% Au, 32 wt% Ag and 20 wt% Cu while SB55 has 45 wt% Au, 30 wt% Ag and 25 wt% Cu.

silver, copper and tin. The data for the standards in table 10 calculated against SB18 were therefore re-calculated this time standardising gold, silver, copper and tin against MAC2. This in many cases revealed a better correlation between the analysed and expected compositions, although the silver was still slightly higher than the expected values.

The composition of the three MAC standards made for the Staffordshire Hoard project was checked by analysing each ten times at x100 magnification to determine whether they matched the composition certified by the manufacturers. The gold, silver, copper and tin in these standards were standardised against each of the three standards separately, i.e. the certified composition of MAC1 was used for standardisation to calculate the quantified data for the analysed composition of MAC1. The data obtained from the three standards by standardising against themselves was then compared to the results obtained against MAC2 (Table 9). Unsurprisingly when standardised against themselves, the calculated quantities were within one standard deviation of the known values. When MAC2 was used for standardising the other MAC standards, there was generally also a good correlation for MAC1. The biggest difference between calculated and certified compositions was seen for MAC3 when standardised against MAC2. This resulted in a higher silver content and therefore lower gold content than expected.

MAC2 and SB18 had compositions that were very close match to the objects chosen for the surface enrichment project. However the MAC2 standard showed the best results for the majority of standards and therefore all SEM-EDX results were calculated with gold, silver, copper and tin being standardised using MAC2, unless otherwise stated. MAC2 was used as the standard regularly analysed by SEM-EDX during the pilot study (Table 7).

	Wt% Au	Wt% Ag	Wt% Cu	Wt% Sn
Certified Value	**74.7**	**19.2**	**5.1**	**1.0**
10/12/2012	74.7	19.2	5.1	1.0
14/12/2012	74.6	19.3	5.3	0.9
08/01/2013	74.6	19.3	5.1	1.0
11/01/2013	74.7	19.3	5.0	1.1
17/01/2013	74.5	19.4	5.1	1.0
28/01/2013	74.6	19.3	5.1	1.0
07/02/2013	74.6	19.4	5.1	1.0

Table 7. SEM-EDX normalised results from regular analysis of MAC2.

	Accepted or Certified Values				BM High Gold Method			BM Base Gold Method			Staffordshire Hoard Method				Staffordshire Hoard High Gold Method				Staffordshire Hoard Mid Gold Method			
Standard	**Wt% Au**	**Wt% Ag**	**Wt% Cu**	**Wt% Sn**	**Wt% Au**	**Wt% Ag**	**Wt% Cu**	**Wt% Au**	**Wt% Ag**	**Wt% Cu**	**Wt% Au**	**Wt% Ag**	**Wt% Cu**	**Wt% Sn**	**Wt% Au**	**Wt% Ag**	**Wt% Cu**	**Wt% Sn**	**Wt% Au**	**Wt% Ag**	**Wt% Cu**	**Wt% Sn**
SB8A	**71.0**	**24.1**	**4.9**	**-**	71.5	23.6	4.9	69.5	25.6	4.9	70.8	24.1	5.1		71.1	23.8	5.1		71.0	24.2	4.8	
SB11	**85.4**	**9.6**	**5.0**	**-**	86.2	9.1	4.7	85.1	10.1	4.8	85.7	9.4	4.9		85.9	9.2	4.9		85.9	9.4	4.7	
SB12	**90.0**	**5.0**	**5.0**	**-**	90.2	5.1	4.7	89.5	5.7	4.8	89.8	5.3	4.9		89.9	5.2	4.9		90.0	5.3	4.7	
SB17	**65.9**	**28.2**	**5.9**	**-**	66.8	27.4	5.8	64.7	29.5	5.8	66.0	27.9	6.0		66.4	27.6	6.0		66.2	28.0	5.8	
SB18	**63.4**	**27.2**	**9.4**	**-**	64.4	26.2	9.4	62.3	28.2	9.5	63.6	26.7	9.7		63.8	26.4	9.8		63.7	26.9	9.4	
SB39	**50.0**	**30.0**	**20.0**	**-**	50.9	28.6	20.5	48.9	30.5	20.6	49.9	28.9	21.1		50.2	28.6	21.2		50.3	29.3	20.4	
BM MAC1	**93.9**	**4.6**	**1.0**	**0.5**	94.6	4.4	1.0	94.1	4.9	1.0	93.8	4.5	1.0	0.7	93.9	4.4	1.0	0.7	94.1	4.5	1.0	0.4
BMT MAC1					94.7	4.3	1.0	94.2	4.8	1.0	94.0	4.5	1.0	0.5	94.1	4.4	1.0	0.5	94.2	4.4	1.0	0.4
Stoke MAC1					94.6	4.4	1.0	94.2	4.8	1.0	94.0	4.5	1.0	0.5	94.1	4.4	1.0	0.5	94.1	4.5	1.0	0.4
BM MAC2	**74.7**	**19.2**	**5.1**	**1.0**	76.3	18.8	4.9	74.5	20.5	5.0	74.7	19.0	5.1	1.2	75.0	18.7	5.1	1.2	75.1	19.1	4.9	0.9
BMT MAC2					76.3	18.9	4.8	74.5	20.6	4.9	74.7	19.2	5.0	1.1	75.0	18.9	5.0	1.1	75.2	19.3	4.8	0.7
Stoke MAC2					76.5	18.9	4.6	74.7	20.6	4.7	75.0	19.3	4.8	0.9	75.4	18.9	4.8	0.9	75.5	19.3	4.6	0.6
BM MAC3	**59.4**	**29.8**	**9.1**	**2**	61.0	30.1	8.9	58.7	32.3	9.0	59.0	30.0	9.1	1.9	59.3	29.6	9.2	1.9	59.6	30.3	8.8	1.3
BMT MAC3					61.1	29.7	9.2	58.8	31.9	9.3	58.9	29.6	9.5	2.0	59.3	29.2	9.5	2.0	59.4	29.9	9.1	1.6
Stoke MAC3					61.2	30.0	8.8	58.9	32.2	8.9	59.1	29.8	9.0	2.1	59.4	29.4	9.1	2.1	59.7	30.2	8.7	1.4

Table 8. Comparison between the compositional data of selected standards using the five different XRF standardisation methods presented above. Each figure is the average of at least four separate analyses carried out on different days, with the exception of SB8A where nine analyses were carried out on different days. The results for the MAC standards are the average of three analyses acquired for 600 seconds all carried out on the same day. Note that the BM High Gold and BM Base Gold methods do not calculate the tin content present, so when tin is present in a sample the totals are normalised and therefore the apparent quantities of the other elements are increased.

		Accepted and Certified Values				Standardised with SB18			*	Standardised with MAC2			
		Wt% Au	Wt% Ag	Wt% Cu	Wt% Sn	Wt% Au	Wt% Ag	Wt% Cu	Wt% Sn	Wt% Au	Wt% Ag	Wt% Cu	Wt% Sn
SB8A	Average	**71.0**	**24.1**	**4.9**		70.4	24.5	5.1		70.4	24.5	5.1	
	Standard Deviation					***0.1***	***0.1***	***0.1***		***0.15***	***0.15***	***0.07***	
SB11	Average	**85.4**	**9.6**	**5.0**		85.1	9.8	5.1		85.2	9.8	5.0	
	Standard Deviation					***0.13***	***0.11***	***0.07***		***0.13***	***0.11***	***0.07***	
SB12	Average	**90.0**	**5.0**	**5.0**		89.4	5.4	5.2		89.4	5.4	5.2	
	Standard Deviation					***0.11***	***0.10***	***0.05***		***0.11***	***0.10***	***0.05***	
SB17	Average	**65.9**	**28.2**	**5.9**		64.7	29.2	6.1		64.8	29.2	6.0	
	Standard Deviation					***0.20***	***0.16***	***0.06***		***0.20***	***0.16***	***0.06***	
SB18	Average	**63.4**	**27.2**	**9.4**		63.4	27.2	9.4		63.4	27.3	9.3	
	Standard Deviation					***0.13***	***0.10***	***0.07***		***0.13***	***0.10***	***0.08***	
SB39	Average	**50.0**	**30.0**	**20.0**		48.9	30.9	20.1		49.0	31.0	20.0	
	Standard Deviation					***0.11***	***0.08***	***0.10***		***0.11***	***0.08***	***0.10***	
MAC1	Average	**93.9**	**4.6**	**1.0**	**0.5**	93.9	4.4	1.1	0.6	94.0	4.4	1.1	0.5
	Standard Deviation					***0.14***	***0.08***	***0.06***	***0.08***	***0.13***	***0.08***	***0.06***	***0.07***
MAC2	Average	**74.7**	**19.2**	**5.1**	**1.0**	74.5	19.2	5.1	1.3	74.6	19.3	5.1	1.0
	Standard Deviation					***0.19***	***0.10***	***0.09***	***0.10***	***0.17***	***0.10***	***0.08***	***0.08***
MAC3	Average	**59.4**	**29.8**	**9.1**	**2.0**	58.3	30.2	9.0	2.5	58.5	30.5	9.0	2.0
	Standard Deviation					***0.21***	***0.18***	***0.06***	***0.11***	***0.21***	***0.18***	***0.06***	***0.08***

Table 9. Comparison between the SEM-EDX compositional data obtained with the standardisation of gold, silver and copper using SB18 and MAC2 and of gold, silver, copper and tin using MAC2 for selected standards. *As there is no tin in SB18, it was not possible to standardise the tin in the MAC standards and therefore for tin MAC2 was used throughout. The results have been normalised and the average of ten analyses and standard deviation of these ten analyses reported.

		Certified Values				Standardised against themselves				Standardised using MAC 2			
		Wt% Au	Wt% Ag	Wt% Cu	Wt% Sn	Wt% Au	Wt% Ag	Wt% Cu	Wt% Sn	Wt% Au	Wt% Ag	Wt% Cu	Wt% Sn
MAC 1	Average	**93.9**	**4.6**	**1.04**	**0.5**	93.9	4.6	1.0	0.5	94.0	4.4	1.1	0.5
	Standard Deviation					***0.11***	***0.08***	***0.06***	***0.06***	***0.13***	***0.08***	***0.06***	***0.07***
MAC 2	Average	**74.7**	**19.2**	**5.1**	**1.0**	74.6	19.3	5.1	1.0	74.6	19.3	5.1	1.0
	Standard Deviation					***0.17***	***0.10***	***0.08***	***0.08***	***0.17***	***0.10***	***0.08***	***0.08***
MAC 3	Average	**59.4**	**29.8**	**9.1**	**2.0**	59.2	29.7	9.1	2.0	58.5	30.5	9.0	2.0
	Standard Deviation					***0.21***	***0.17***	***0.06***	***0.09***	***0.21***	***0.18***	***0.06***	***0.08***

Table 10. Comparison between the SEM-EDX compositional data of the BM MAC standards obtained with the standardisation of gold, silver, copper and tin using each standard respectively (i.e. each standard is standardised against itself) and then standardised using MAC2. The results have been normalised and the average of ten analyses and standard deviation of these ten analyses reported.

Comparison between XRF and SEM analyses of selected standards

The compositional data of all three MAC standards from each of the three commissioned sets (BM, BMT and PMAG) analysed by both XRF and SEM-EDX were compared (Table 11).

The data for the three MAC1 standards gave no significant differences between the three sets. Further, the compositional data determined using XRF and SEM-EDX were closely similar to each other and well within any expected errors produced by the instruments themselves.

The data for the MAC2 standards revealed a possible slight difference in the copper and tin contents but generally good agreement was obtained using both analytical techniques. Comparison between XRF and SEM-EDX data suggests that, while XRF seems to underestimate the silver content, SEM-EDX appears to slightly overestimate it.

The MAC3 standards show the biggest inconsistencies between the three sets. SEM-EDX analysis indicates a relatively large difference between the silver and tin contents, with MAC3 from PMAG being richer in silver and poorer in tin and copper, and MAC3 from BMT being poorer in silver and richer in tin and copper. The XRF results appear more consistent with the certified values, although there are some differences in the copper content, and there is a much bigger standard deviation across the three standards compared to the sets of MAC 1 and 2 standards. These differences in composition are most likely related to the heterogeneity of the standards as SEM-EDX area analyses are very reproducible, and may reflect how the standards were produced. Heterogeneity is commonly seen in low carat gold objects (Dugmore and DesForges 1979). For MAC3, there were also some differences between the SEM-EDX and XRF results; typically SEM-EDX analysis results in a higher silver content, and therefore lower gold content.

Standard			Certified Values				XRF Analysis				SEM-EDX Analysis			
			Wt% Au	Wt% Ag	Wt% Cu	Wt% Sn	Wt% Au	Wt% Ag	Wt% Cu	Wt% Sn	Wt% Au	Wt% Ag	Wt% Cu	Wt% Sn
MAC 1	BM	Average	93.9	4.6	1.0	0.5	93.9	4.4	1.0	0.7	94.0	4.4	1.1	0.5
		Standard Deviation					***0.30***	***0.12***	***0.01***	***0.20***	***0.13***	***0.08***	***0.06***	***0.07***
	BMT	Average					94.1	4.4	1.0	0.5	93.6	4.6	1.4	0.4
		Standard Deviation					***0.10***	***0.06***	***0.02***	***0.04***	***0.10***	***0.09***	***0.04***	***0.09***
	PMAG	Average					94.1	4.4	1.0	0.5	93.7	4.5	1.3	0.5
		Standard Deviation					***0.19***	***0.01***	***0.03***	***0.21***	***0.06***	***0.05***	***0.04***	***0.10***
MAC 2	BM	Average	74.7	19.2	5.1	1.0	75.0	18.7	5.1	1.2	74.6	19.3	5.1	1.0
		Standard Deviation					***0.21***	***0.18***	***0.02***	***0.21***	***0.17***	***0.10***	***0.08***	***0.08***
	BMT	Average					75.0	18.9	5.0	1.1	74.3	19.6	5.1	1.0
		Standard Deviation					***0.03***	***0.07***	***0.10***	***0.05***	***0.11***	***0.10***	***0.06***	***0.09***
	PMAG	Average					75.4	18.9	4.8	0.9	74.4	19.9	4.8	0.9
		Standard Deviation					***0.13***	***0.08***	***0.02***	***0.13***	***0.08***	***0.07***	***0.05***	***0.06***
MAC 3	BM	Average	59.4	29.8	9.1	2.0	59.3	29.6	9.2	1.9	58.5	30.5	9.0	2.0
		Standard Deviation					***0.16***	***0.15***	***0.14***	***0.15***	***0.21***	***0.18***	***0.06***	***0.08***
	BMT	Average					59.3	29.2	9.5	2.0	58.3	29.6	9.9	2.2
		Standard Deviation					***0.15***	***0.19***	***0.06***	***0.19***	***0.09***	***0.44***	***0.28***	***0.23***
	PMAG	Average					59.4	29.4	9.1	2.1	58.0	31.9	8.5	1.6
		Standard Deviation					***0.08***	***0.28***	***0.14***	***0.23***	***0.13***	***0.25***	***0.15***	***0.12***

Table 11. Certified composition of the Staffordshire Hoard standards compared to XRF and SEM-EDX results. The results have been normalised. The XRF results are the average of three analyses carried out on the same day and the SEM-EDX results are the average of at least three analyses.

Six of the SB standards manufactured and used at the BM were also analysed by both XRF and SEM-EDX and their data compared (Table 12). XRF analysis tended to give lower silver contents for most of the standards, the only exception being SB12. The copper content was generally within a couple of standard deviations of the accepted composition. There were two major exceptions: SB18 which was within two standard deviations of the accepted

composition, and SB39 which had a higher copper content when analysed by XRF. The results for SB39 would have been improved if another XRF standardisation method (i.e. if the Staffordshire Hoard Mid Gold Method) or, for the SEM-EDX, if a standard with higher silver and copper content had been used for standardisation. The SEM-EDX results were generally higher in silver, and therefore lower in gold, than the expected values and the XRF data. With SEM-EDX the copper was usually within one standard deviation of the known composition, with the exception of SB12 (Table 12).

Standard		Known Composition			XRF Analysis			SEM-EDX Analysis		
		Wt% Au	Wt% Ag	Wt% Cu	Wt% Au	Wt% Ag	Wt% Cu	Wt% Au	Wt% Ag	Wt% Cu
SB8A	Average	71.0	24.1	4.9	71.1	23.8	5.1	70.4	24.5	5.1
	Standard Deviation				***0.22***	***0.22***	***0.05***	***0.15***	***0.15***	***0.07***
SB11	Average	85.4	9.6	5.0	85.9	9.2	4.9	85.2	9.8	5.0
	Standard Deviation				***0.26***	***0.25***	***0.04***	***0.13***	***0.11***	***0.07***
SB12	Average	90.0	5.0	5.0	89.9	5.2	4.9	89.4	5.4	5.2
	Standard Deviation				***0.16***	***0.13***	***0.10***	***0.11***	***0.10***	***0.05***
SB17	Average	65.9	28.2	5.9	66.4	27.6	6.0	64.7	29.3	6.0
	Standard Deviation				***0.13***	***0.19***	***0.06***	***0.20***	***0.16***	***0.06***
SB18	Average	63.4	27.2	9.4	63.8	26.4	9.8	63.4	27.3	9.3
	Standard Deviation				***0.21***	***0.41***	***0.20***	***0.13***	***0.10***	***0.08***
SB39	Average	50.0	30.0	20.0	50.2	28.6	21.2	49.0	31.0	20.0
	Standard Deviation				***0.13***	***0.11***	***0.11***	***0.11***	***0.08***	***0.10***

Table 12. Known compositions of the BM SB standards used for this study compared to the XRF and SEM-EDX data. All XRF results are an average of four analyses carried out on separate days, with the exception of SB8A where nine analyses were carried out. The SEM results are an average of 10 analyses at 100x magnification.

There is some small variation between the observed values for the standards selected when analysed by the British Museum XRF and SEM-EDX, and the expected or certified values of the standards. Despite this, the variation observed remains within acceptable limits, as they are smaller than the compositional differences in objects discussed in the enrichment report and well within any expected errors produced by the instruments themselves..

Appendix 4 – XRF Experiments

A number of experiments were carried out to optimise the parameters to be used to collect the data on each instrument. Several tests were carried out on the XRF, the first of which was to determine how precise the results were by repeating the same analysis on the same area of a standard. As this pilot study required a smaller beam size for several analyses, the effect of the collimator size, and therefore beam size, on the collection time required for an accurate result was also studied. Finally, the effect of changing the working distance and the possible errors introduced by the geometry of the object were jointly tested.

The XRF calculation software uses specific energy peaks to calculate the totals for each element; these are listed in table 13 below.

	XRF
Gold	Lα
Silver	Kα
Copper	Kα
Tin	Kβ

Table 13. List of the different peaks used by XRF and energy lines used by the SEM-EDX to calculate totals for each element.

All these experiments are meant to provide guidance, as they were only carried out once and on a selection of standards relevant to the Staffordshire Hoard research project. To produce more reliable data, they would need to be repeated multiple times on different standards but this was beyond the scope of this project.

Precision

Multiple analyses of the same area of standard SB8A were carried out to determine the precision[8] of the XRF instrument for alloys of this composition. This revealed that there was good internal consistency, with a standard deviation[9] of only ±0.25% for gold and silver and under ±0.1% for copper (Table 14) between all ten analyses. There was similar variability in standard deviations when the analyses of SB8A from across ten different days were examined, although in this case the silver content was lower than the accepted composition which most likely reflects the heterogeneity of the standard. This is within the acceptable errors quoted by Cowell (1998) for the precision which is ±0.5% for majors.

[8] Precision is the ability of a measurement to be consistently reproduced.

[9] Standard deviation is a statistic used as a measure of the dispersion or variation from the mean in a distribution. In a normal distribution one standard deviation of the mean includes 65% of the results, two standard deviations include 95% and three standard deviations include 99%.

Carried out on the same day, in the same area				Carried out on different days, in different areas			
	Wt% Au	Wt% Ag	Wt% Cu		Wt% Au	Wt% Ag	Wt% Cu
1	71.0	23.8	5.2	08/02/2013	71.0	23.9	5.1
2	70.8	24.0	5.2	07/02/2013	70.9	24.0	5.1
3	71.2	23.6	5.2	17/10/2012	71.3	23.7	5.0
4	70.7	24.1	5.2	15/11/2012	71.3	23.6	5.1
5	70.8	24.1	5.1	08/02/2013	71.0	23.9	5.1
6	70.7	24.2	5.1	12/02/2013	71.2	23.7	5.1
7	70.4	24.5	5.1	14/02/2013	70.8	24.1	5.1
8	71.0	23.8	5.2	15/02/2013	71.3	23.6	5.1
9	70.7	24.1	5.2	19/02/2013	71.2	23.7	5.1
10	70.6	24.2	5.2	01/03/2013	71.0	23.8	5.2
Average	**70.8**	**24.0**	**5.2**		**71.1**	**23.8**	**5.1**
Standard Deviation	***0.23***	***0.25***	***0.05***		***0.18***	***0.17***	***0.05***
SB8A Accepted	**71.0**	**24.1**	**4.9**		**71.0**	**24.1**	**4.9**

Table 14. Repeated analysis of SB8A to determine the precision of the XRF instrument.

Collimator Size

During the pilot enrichment study, it was necessary to change collimator to reduce the size of the beam, in order to be able to analyse the small sub-surface area exposed or smaller features on artefacts. This reduces the area of the incident X-ray beam and hence the total number of X-ray photons emitted by the sample and reaching the detector, when using the 0.2 mm instead of the 0.65 mm collimator the number of counts is decreased by *c*. 11 times. Therefore to determine the effect of the different collimators on the acquisition time required to give accurate and precise data, an experiment was carried out using SB8A. The first test was carried out with the 0.65 mm collimator at 500 µA, the second with the 0.2 mm collimator at 500 µA and the third with the 0.2 mm collimator at 700 µA, increasing the current in an attempt to off-set the loss of incident photons with the smaller collimator.

	0.65 mm collimator, 500µmA			0.2 mm collimator, 500µmA			0.2 mm collimator, 700µmA		
Count Time	**Wt% Au**	**Wt% Ag**	**Wt% Cu**	**Wt% Au**	**Wt% Ag**	**Wt% Cu**	**Wt% Au**	**Wt% Ag**	**Wt% Cu**
200	71.1	23.8	5.1	71.4	23.3	5.3	71.6	23.1	5.3
400	70.9	24.0	5.1	70.3	24.5	5.2	70.8	24.1	5.1
600	71.0	23.9	5.1	71.6	23.3	5.1	71.4	23.6	5.0
1200	70.8	24.1	5.1	70.9	23.9	5.2	71.2	23.7	5.1
2400	70.7	24.2	5.1	71.2	23.6	5.2	70.8	24.0	5.2
Average	***70.9***	***24.0***	***5.1***	***71.1***	***23.7***	***5.2***	***71.2***	***23.7***	***5.1***
Standard Deviation	***0.15***	***0.16***	***0.01***	***0.5***	***0.49***	***0.7***	***0.37***	***0.41***	***0.09***
Accepted SB8A	**71.0**	**24.1**	**4.9**	**71.0**	**24.1**	**4.9**	**71.0**	**24.1**	**4.9**

Table 15. Data from the experiment investigating the acquisition time required for reliable analysis when using the small 0.2 mm collimator compared to the 0.65 mm collimator. The results have been normalised.

Figure 17 and table 15 suggest that the error produced by using a small collimator with shorter acquisition times does not appear to be very significant for major elements. The gold and silver contents even with short acquisition times are usually within two or three standard deviations of the expected standard composition, resulting in potential errors of up to 0.5%. These errors are therefore not significant, particularly when undertaking surface analysis where the data is only semi-quantitative. Acquiring data for 600 seconds is however much more likely to give more accurate results than 200 seconds, as with such an acquisition time (or greater), all lines tend to come closer to the average dotted line thus reducing the discrepancy between them, to the point that the error is minimised. The effect of increasing

the current was minimal on the results, but it did increase the running temperature of the instrument.

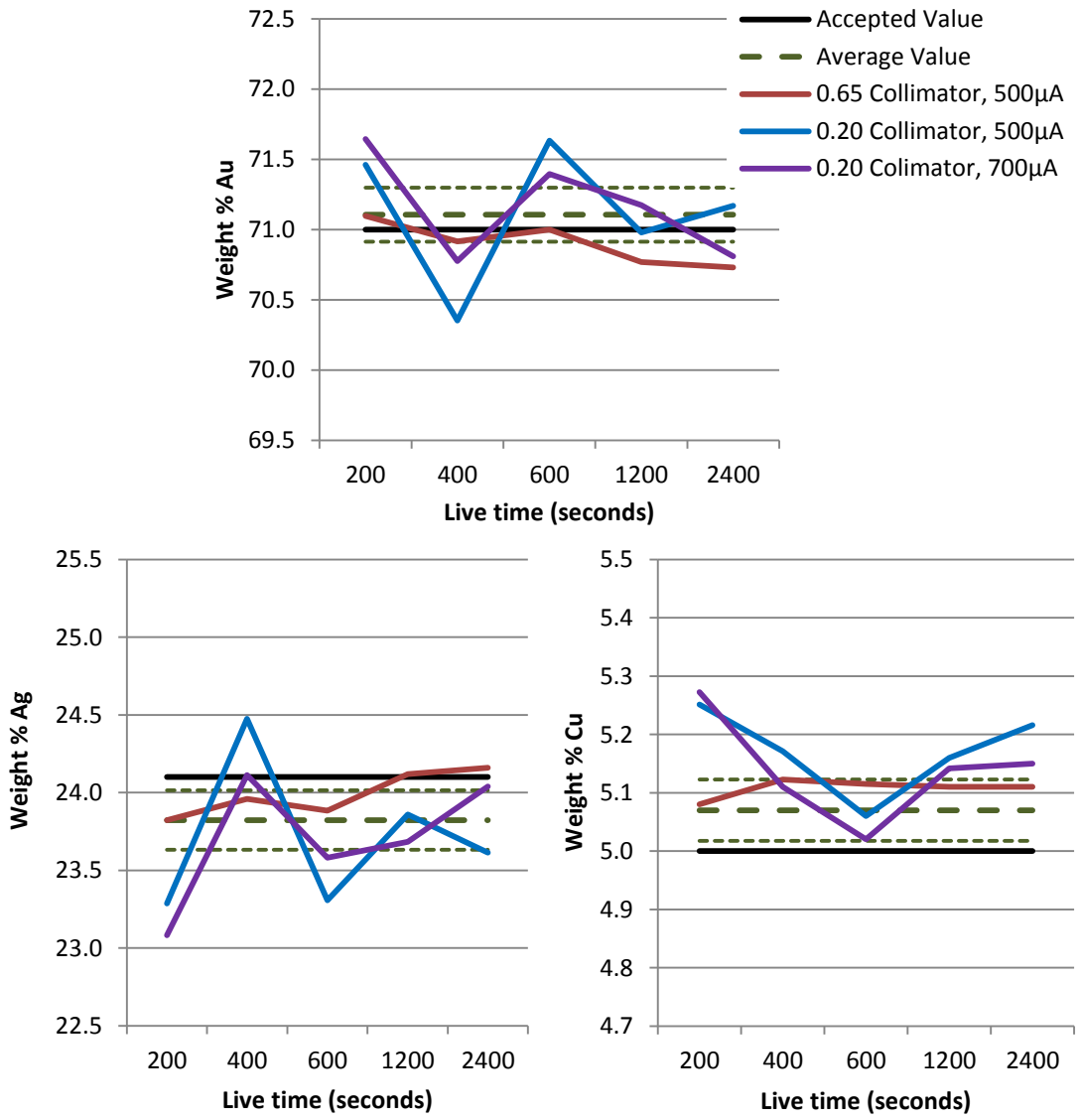

Figure 17. Graphs showing the detected weight percentages of gold, silver and copper depending on the XRF collimator sizes. The thick dashed line is the average of nine analyses of SB8A over several days collected for 200 seconds with the 0.65 mm collimator. The thinner dashed lines show one standard deviation from this average.

Working Distance

The working distance is the pre-set distance for reproducibility between the beam generator, the detector and the sample and will be different depending on each instrument. The working distance and height will be referred to as the z-axis.

To investigate the potential error produced by variations in the working distance (z-axis) a number of analyses on standard SB8A were undertaken. The XRF stage was mechanically moved on the z-axis closer to, and then further away from the optimal analytical working distance. Figure 18 and table 16 show that, for up to 0.5 mm either side of the focal point,

the results are usually within one standard deviation of the calculated average of the standard. This suggests that whenever possible optimal working distance should be used but small differences in artefact height do not necessarily result in a large errors.

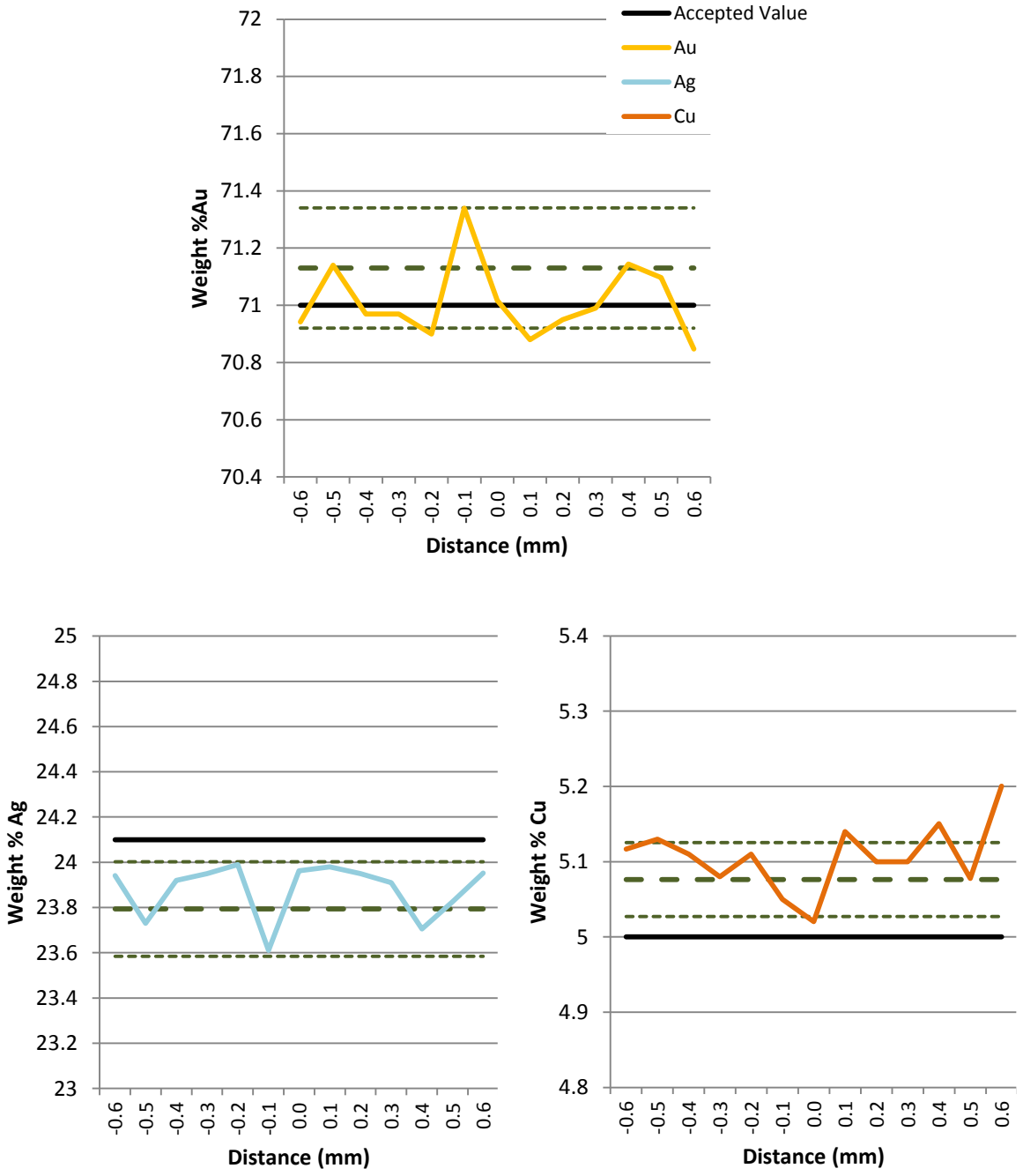

Figure 18. Graphs showing the variations in concentrations of gold, silver and copper with the working distance (z-axis) when using the XRF. The optimum working distance is indicated at 0.0 mm, the negative distances represent moving the standard closer to the detector while the positive distances reflect an increase in the distance between the detector and the sample. The thick dashed line is the average of nine analyses of SB8A over several days collected for 200 seconds with the 0.65 mm collimator. The thinner dashed lines show the standard deviation from this average.

Distance	Wt% Au	Wt% Ag	Wt% Cu
-0.6 mm	70.9	23.9	5.12
-0.5 mm	71.1	23.7	5.13
-0.4 mm	71.0	23.9	5.11
-0.3 mm	71.0	24.0	5.08
-0.2 mm	70.9	24.0	5.11
-0.1 mm	71.3	23.6	5.05
0.0 mm	71.0	24.0	5.02
0.1 mm	70.9	24.0	5.14
0.2 mm	71.0	24.0	5.10
0.3 mm	71.0	23.9	5.10
0.4 mm	71.1	23.7	5.15
0.5 mm	71.1	23.8	5.08
0.6 mm	70.8	24.0	5.20
Average	***71.0***	***23.9***	***5.1***
Standard Deviation	***0.13***	***0.12***	***0.05***
Expected SB8A	**71.0**	**24.1**	**4.9**

Table 16. Data from the experiment investigating the effect of analysing at different working distances. The results have been normalised.

Geometry

A further consideration when analysing objects using the XRF is whether the geometry of the surface of the object in relation to the detector will affect the results. An experiment was therefore carried out on one of the Staffordshire Hoard artefacts, pommel cap K88. This was chosen as its top surface was clean and it had a domed symmetrical shape, which can be seen at the top of figure 21. Several point analyses were carried out across the x-axis and y-axis of the object, at 0.5 mm intervals, in each case the working distance was re-adjusted. The y-axis runs parallel to the detector (Figure 19).

Figure 19. Photograph of the top and side of pommel cap K88 showing the spatial relationship between the object, the XRF detector and incident X-ray beam. The plane horizontal and vertical axes will be referred to as x-axis and y-axis respectively.

While the results shown in figure 21 indicate that perfectly flat surfaces are ideal and give the best results;[10] small changes in the angle (*c.* ±5º) between the object and detector still remain within one standard deviation of the average. Other researchers have suggested that a tilt in the object surface up to 30° from the horizontal can lead to ±5% relative error, and a tilt of 60° up to ±10% error (Cowell 1977; Stern 1995). This experiment demonstrates that only with extreme changes in object shape (above ±30º) do the gold and silver compositions change dramatically. Copper on the other hand appears to be dramatically affected by the degree of tilt and therefore by object geometry in the x-axis but is less affected in the y-axis. This relates to the location of the detector on this equipment and to the geometry of the object (Figure 20). When analysing the top centre of K88, the photons emitted can easily escape the gold alloy and this remains the case as the take-off angle increases (Figures 16 and 20). However as the take-off angle becomes shallower (Figures 16 and 20), and part of the object starts to block the emitted X-rays, the photons have to travel through more of the gold alloy which will absorb the lower energy X-rays preferentially before reaching the detector. This results in the reduction of copper seen in figure 21. This effect may also be expected whenever any material is between the detector and point being analysed. The results, for this instrumental configuration, suggest that movement in the y-axis, parallel with the detector will reduce this effect.

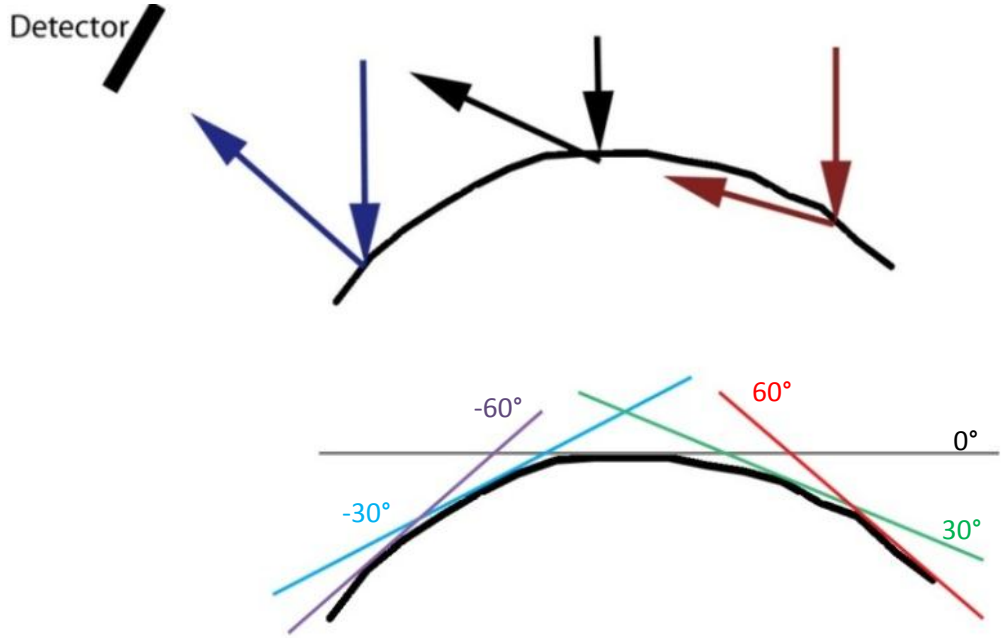

Figure 20. Geometry of the object on the x-axis showing where the X-ray beam hits the object, and where the ejected photons travel. The bottom image the gives the estimated angles of the surface of the object.

[10] In this experiment the stage could be moved in mm increments hence the measurements in the following figures and tables but the error produced is being compared to the shape and geometry of the object, this can be seen at the top of Figure 21.

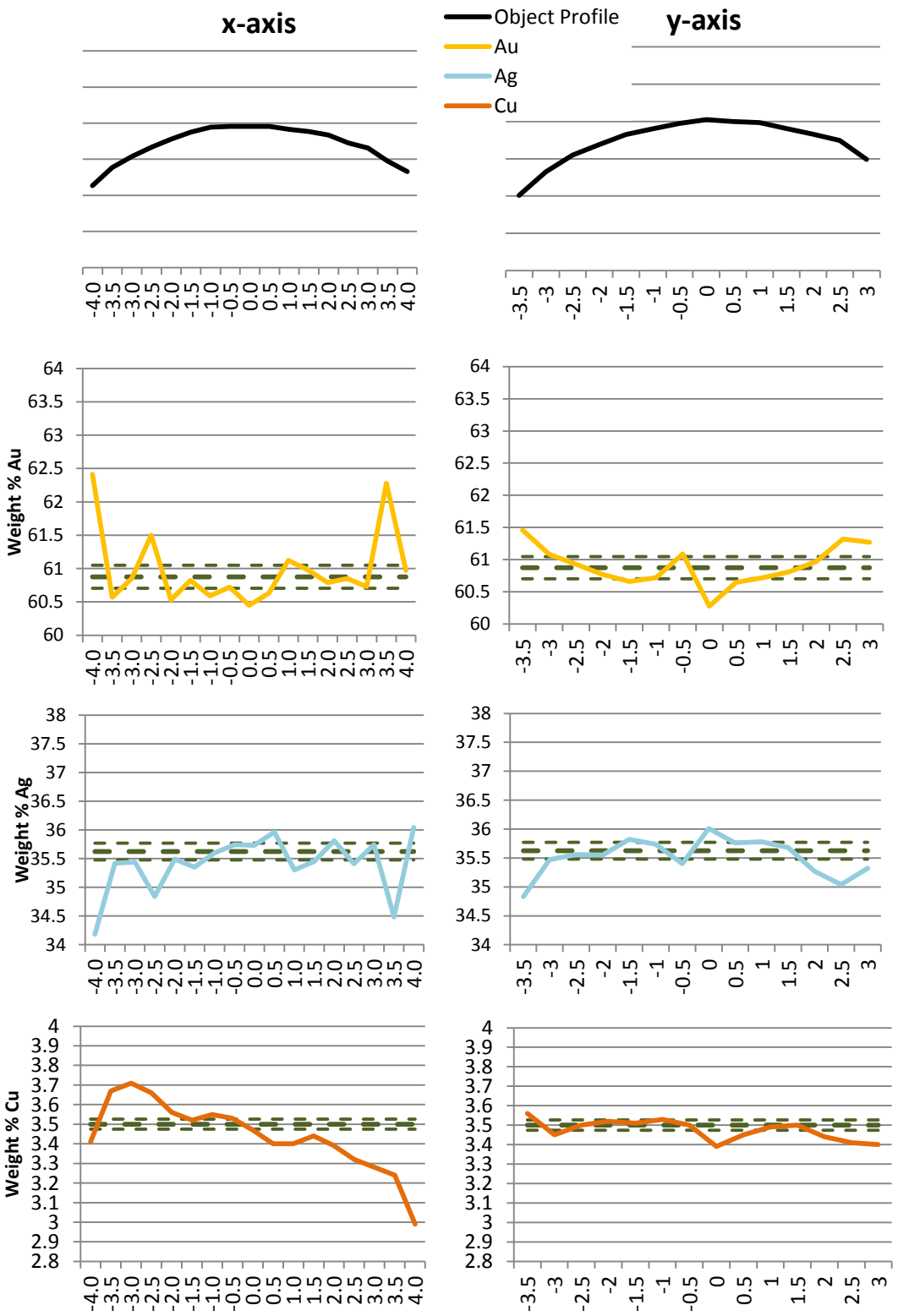

Figure 21. Graphs showing the variations in concentrations of gold, silver and copper measured depending on the angle of the object surface (seen in the top chart) in relation to the detector, when using the XRF. It also shows how the angle of the X-ray beam and the detector interacts with the geometry of the object. The thick dashed line is the average of three analyses at the flat top of pommel K88 collected for 200 seconds with the 0.65 mm collimator. The thinner dashed lines show the standard deviation from this average.

Position	Distance	x-axis				y-axis			
		Height mm	Wt% Au	Wt% Ag	Wt% Cu	Height mm	Wt% Au	Wt% Ag	Wt% Cu
1	-4.0 mm	23.27	62.4	34.2	3.4				
2	-3.5 mm	23.77	60.8	35.5	3.7	23.02	61.5	34.9	3.6
3	-3.0 mm	24.08	60.9	35.4	3.7	23.65	61.0	35.5	3.5
4	-2.5 mm	24.33	61.5	34.8	3.7	24.10	60.9	35.6	3.5
5	-2.0 mm	24.56	60.8	35.6	3.6	24.38	60.9	35.6	3.5
6	-1.5 mm	24.75	61.0	35.5	3.5	24.65	60.7	35.8	3.5
7	-1.0 mm	24.89	60.7	35.7	3.6	24.80	60.8	35.7	3.5
8	-0.5 mm	24.91	60.8	35.7	3.5	24.95	61.1	35.4	3.5
9	0.0 mm	24.91	60.6	35.9	3.5	25.05	60.5	36.1	3.4
10	0.5 mm	24.91	60.6	36.0	3.4	25.00	60.7	35.8	3.5
11	1.0 mm	24.83	61.2	35.4	3.4	24.97	60.7	35.8	3.5
12	1.5 mm	24.77	61.1	35.5	3.4	24.81	60.8	35.7	3.5
13	2.0 mm	24.67	60.8	35.8	3.4	24.66	61.1	35.4	3.5
14	2.5 mm	24.45	61.1	35.6	3.3	24.49	61.5	35.1	3.4
15	3.0 mm	24.31	60.9	35.8	3.3	23.98	61.3	35.3	3.4
16	3.5 mm	23.95	62.3	34.5	3.2				
17	4.0 mm	23.66	61.0	36.0	3.0				
Average of all analyses			**61.0**	**35.4**	**3.4**		**60.9**	**35.5**	**3.5**
Standard Deviation of all analyses			*0.57*	*0.50*	*0.18*		*0.33*	*0.32*	*0.05*
Average of 6-12 centre analyses			**60.8**	**35.6**	**3.5**		**60.7**	**35.7**	**3.5**
Standard Deviation of 6-12 centre analyses			*0.23*	*0.24*	*0.09*		*0.22*	*0.18*	*0.05*
Average of 3 K88			***60.9***	***35.6***	***3.5***		***60.9***	***35.6***	***3.5***
Standard Deviation			*0.17*	*0.15*	*0.03*		*0.17*	*0.15*	*0.03*

Table 17. Data from the experiment investigating the effect of geometry on the XRF compositional data. The results have been normalised.

Appendix 5 – SEM-EDX Experiments

Tests were also run on the SEM-EDX, the first of which was to determine the effect of the working distance on the results, since not all the objects could be safely analysed at the optimum working distance because of their irregular shape. Comparison between standards run in high vacuum and low vacuum was also carried out. The final experiment examined the effect of the geometry of the object on the SEM-EDX data and any errors this might potentially introduce during analysis.

Specific energy lines can be selected in the SEM-EDX INCA software to calculate the totals for each element; these are listed in Table 18 below.

	SEM-EDX
Gold	L
Silver	L
Copper	K
Tin	L

Table 18. List of the different peaks used by XRF and energy lines used by the SEM-EDX to calculate totals for each element.

All these experiments are meant to provide guidance, as they were only carried out once and on a selection of standards relevant to the Staffordshire Hoard research project. To produce more reliable data, they would need to be repeated multiple times on different standards but this was beyond the scope of this project.

Working Distance

The working distance is the pre-set distance for reproducibility between the beam generator, the detector and the sample and will be different depending on each instrument. The working distance and height will be referred to as the z-axis. Due to the shape of some of the Staffordshire Hoard objects, it was difficult and, in some cases impossible, to safely analyse exactly the same locations, analysed using the XRF, at the optimal working distance of 10 mm in the British Museum's SEM-EDX. In addition to being an important part of the pilot study, this would particularly be important for the comparison between the PIXE analyses carried out at the Centre de Recherche des Musées de France (C2RMF) in Paris, the XRF analysis undertaken at BMT and both the XRF and SEM-EDX analyses carried out at the BM (Blakelock forthcoming).

Two standards (SB12 and SB17) were analysed using the SEM-EDX at three different working distances: 10 mm, 15 mm and 20 mm. This was to determine its potential effect on the analytical results and estimate any potential error. In each case, three areas were analysed. The results obtained at different working distances have shown that only a small error resulted (Table 19). The detected copper content remains stable as the working distance increases. The main difference is in the silver content which increases as the gold content decreases, which is most likely due to the use of the lower energy L line for silver by the quantification software. Even so the variation produced by the working distance is within acceptable limits because these errors are smaller than the compositional differences expected in the objects.

Working Distance		SB12			SB17		
		Wt% Au	Wt% Ag	Wt% Cu	Wt% Au	Wt% Ag	Wt% Cu
Accepted Values		90	5	5	65.9	28.2	5.9
10mm	Average 10	90.0	5.0	5.0	66.0	28.1	5.9
	Standard Deviation	*0.10*	*0.09*	*0.05*	*0.19*	*0.16*	*0.06*
15mm	Average 3	89.8	5.3	4.9	65.7	28.5	5.8
	Standard Deviation	*0.06*	*0.03*	*0.05*	*0.16*	*0.12*	*0.05*
20mm	Average 3	89.8	5.3	4.9	65.2	29.0	5.8
	Standard Deviation	*0.06*	*0.03*	*0.05*	*0.22*	*0.19*	*0.03*

Table 19. Standards showing the effect of changing the SEM-EDX working distance on the detected composition. In each case, the results were standardised using the same standard analysed at a 10 mm working distance (i.e. SB12 was used to standardise SB12), to remove any error created by the standardisation against another standard. The results have been normalised and the average of ten analyses and standard deviation of these ten analyses reported.

High or Low Vacuum

The PMAG MAC standards were mounted in resin by the manufacturer at the request of the owners. Normally these would be carbon coated to reduce the charging effect caused by the non-conducting resin, but they could not be carbon coated. It was therefore necessary to use the variable pressure SEM at low vacuum (30 Pa) when analysing these samples. In addition low pressure would also be required when analysing objects with attached organic components, therefore to ensure that no errors were introduced due to the gases present in the chamber at low vacua, analyses of the MAC standards held at BM were carried out both in high and low vacua. This revealed that the use of low pressure in the SEM-EDX does not alter the detected concentrations (Table 20).

Standard		Certified Values				High Vacuum (<1 Pa)				Low Vacuum (30 Pa)			
		Wt% Au	Wt% Ag	Wt% Cu	Wt% Sn	Wt% Au	Wt% Ag	Wt% Cu	Wt% Sn	Wt% Au	Wt% Ag	Wt% Cu	Wt% Sn
MAC 1	Average of 3	93.9	4.6	1.04	0.5	94.0	4.4	1.1	0.5	94.0	4.4	1.1	0.5
	Standard Deviation					*0.13*	*0.08*	*0.06*	*0.07*	*0.12*	*0.06*	*0.03*	*0.10*
MAC 2	Average of 3	74.7	19.2	5.1	1.0	74.6	19.3	5.1	1.0	74.7	19.3	5.0	1.0
	Standard Deviation					*0.17*	*0.10*	*0.08*	*0.08*	*0.10*	*0.09*	*0.08*	*0.09*
MAC 3	Average of 3	59.4	29.8	9.1	2	58.5	30.5	9.0	2.0	58.5	30.5	9.0	2.0
	Standard Deviation					*0.21*	*0.18*	*0.06*	*0.08*	*0.10*	*0.07*	*0.06*	*0.06*

Table 20. Compositional data of the three BM MAC standards under both high and low vacua in the SEM-EDX. The results have been normalised and the average of at least three analyses and standard deviation of these analyses reported.

Geometry

For the experiments on geometry, the plane horizontal and vertical axes will be referred to as x-axis and y-axis respectively. The x-axis is perpendicular to (in line with) the detector, Figure 24.

A further consideration when using the SEM, like the XRF, is whether the changes in the surface of the object in relation to the position of the detector will affect the results. A similar experiment was therefore carried out on pommel cap K88. A line of point analyses across the object along the x- and y-axes were carried out (Figure 22). However, unlike with the XRF, it was not possible to re-adjust the working distance for each measurement to

compensate for the topography of the artefact which can be seen at the top of figure 2. The working distance therefore varied between 10 mm and 15 mm, and this change in working distance may have contributed slightly too any errors produced, although the working distance experiment above suggests this would be minimal.

As with the XRF, the SEM-EDX analysis of the very top of the pommel cap resulted in a consistent composition within one standard deviation. The biggest differences seen were when the tilt or angle[11] of the object surface was larger than 30º from horizontal resulting in a take-off angle larger than the SEM-EDX optimum of 35º. This resulted in a drop in silver content and an increase in the gold content. As with the XRF analysis, the copper content remained relatively stable throughout, Figure 23.

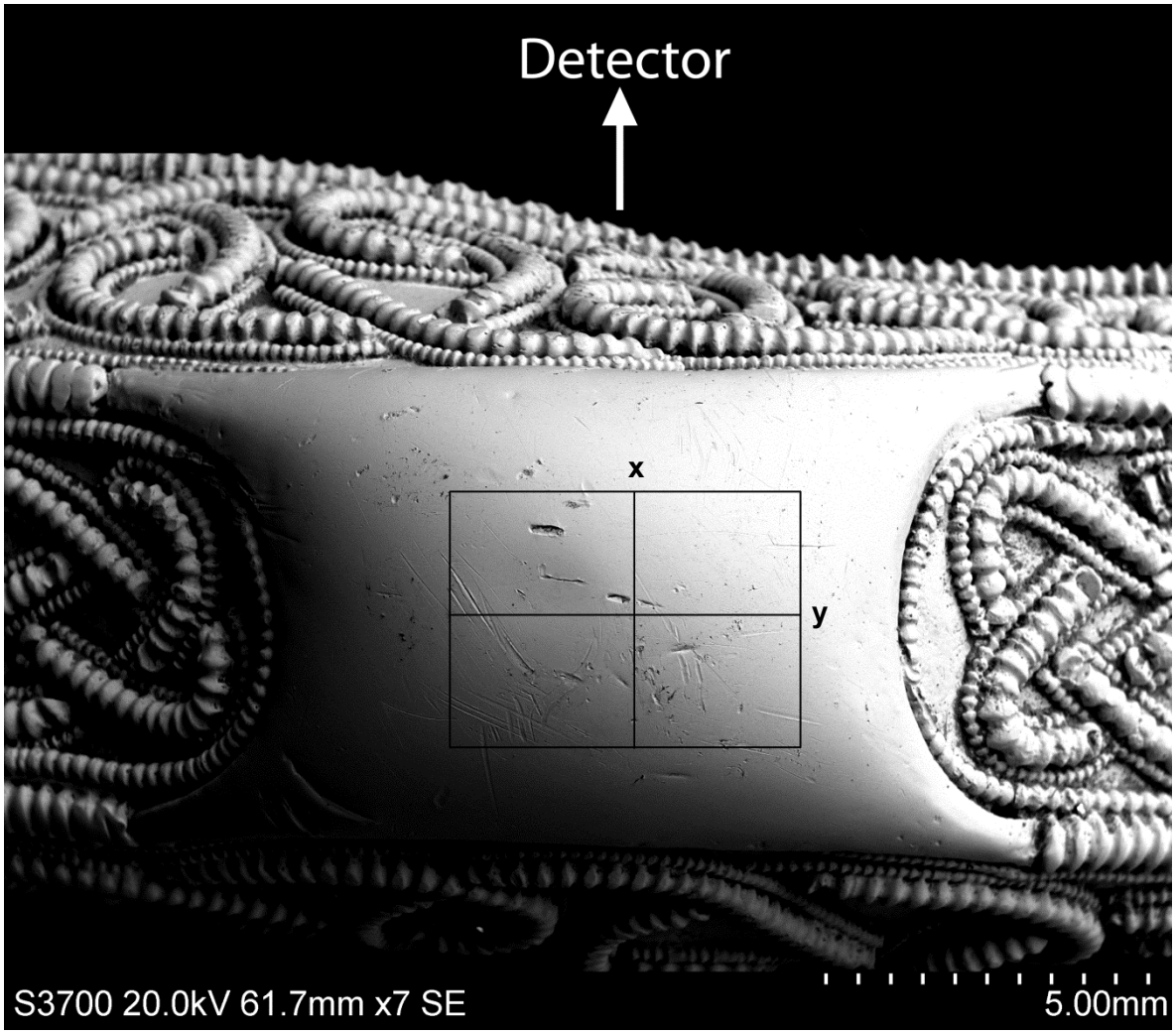

Figure 22. SEM secondary electron image of the top of pommel cap K88. The box shows the area available for analysis at the working distance of 10 mm. The two lines show the x and y axes examined and their relationship to the position of the SEM-EDX detector.

Analysis along the x-axis, perpendicular to the detector, seemed to lead to poor results (Figure 23 and Table 21). Only the very flat top of the pommel produced reliable results. As the angle of the object surface changed, the silver and gold concentrations also changed

[11] In this experiment the stage could be moved in mm increments hence the measurements in the following figures and tables but the error produced is being compared to the shape and geometry of the object, this can be seen at the top of Figure 23.

significantly. This is most likely due to the location of the detector in relation to the object surface where the incident electron beam hits the analysed area, and is therefore related to change in the take-off angle. The silver composition may be more affected due to the lower energy L line being used to calculate the silver content. Overall this experiment showed that the SEM-EDX was more affected by small changes in geometry than the XRF, particularly along the x-axis. However, as with the XRF, the variation is dependent on the location of the detector and the surface being analysed.

		x-axis			y-axis		
Position	**Distance**	**Wt% Au**	**Wt% Ag**	**Wt% Cu**	**Wt% Au**	**Wt% Ag**	**Wt% Cu**
1	-2.33 mm	62.3	34.3	3.5			
2	-2.00 mm	59.6	37.4	3.0			
3	-1.66 mm	60.2	36.8	3.0	57.0	39.8	3.2
4	-1.33 mm	59.8	37.1	3.1	57.2	39.5	3.3
5	-1.00 mm	60.1	36.8	3.1	58.3	38.4	3.3
6	-0.66 mm	59.8	36.9	3.3	58.7	38.4	2.9
7	-0.33 mm	60.6	36.0	3.4	59.6	36.9	3.4
8	0.00 mm	59.8	36.9	3.3	60.3	36.4	3.3
9	0.33 mm	61.0	35.8	3.3	61.1	35.6	3.3
10	0.66 mm	59.7	37.0	3.3	63.0	33.6	3.4
11	1.00 mm	59.8	36.9	3.3	63.9	32.7	3.5
12	1.33 mm	60.4	36.2	3.4	65.9	30.5	3.6
13	1.66 mm	61.1	35.7	3.2	68.1	28.6	3.3
14	2.00 mm	61.2	35.7	3.2	74.0	22.8	3.2
15	2.33 mm	61.5	35.3	3.1			
16	2.66 mm	62.3	34.4	3.3			
17	3.00 mm	63.8	33.0	3.2			
Average of all analyses		**60.8**	**36.0**	**3.2**	**62.3**	**34.4**	**3.3**
Standard Deviation of all analyses		*1.18*	*1.20*	*0.14*	*5.07*	*5.10*	*0.17*
Average of 8-12 centre analyses		**60.1**	**36.6**	**3.3**	**60.5**	**36.2**	**3.3**
Standard Deviation of 8-12 *centre analyses*		*0.56*	*0.56*	*0.06*	*1.63*	*1.76*	*0.20*

Table 21. Data from the experiment investigating the effect of geometry on the SEM-EDX analytical data. The results have been normalised.

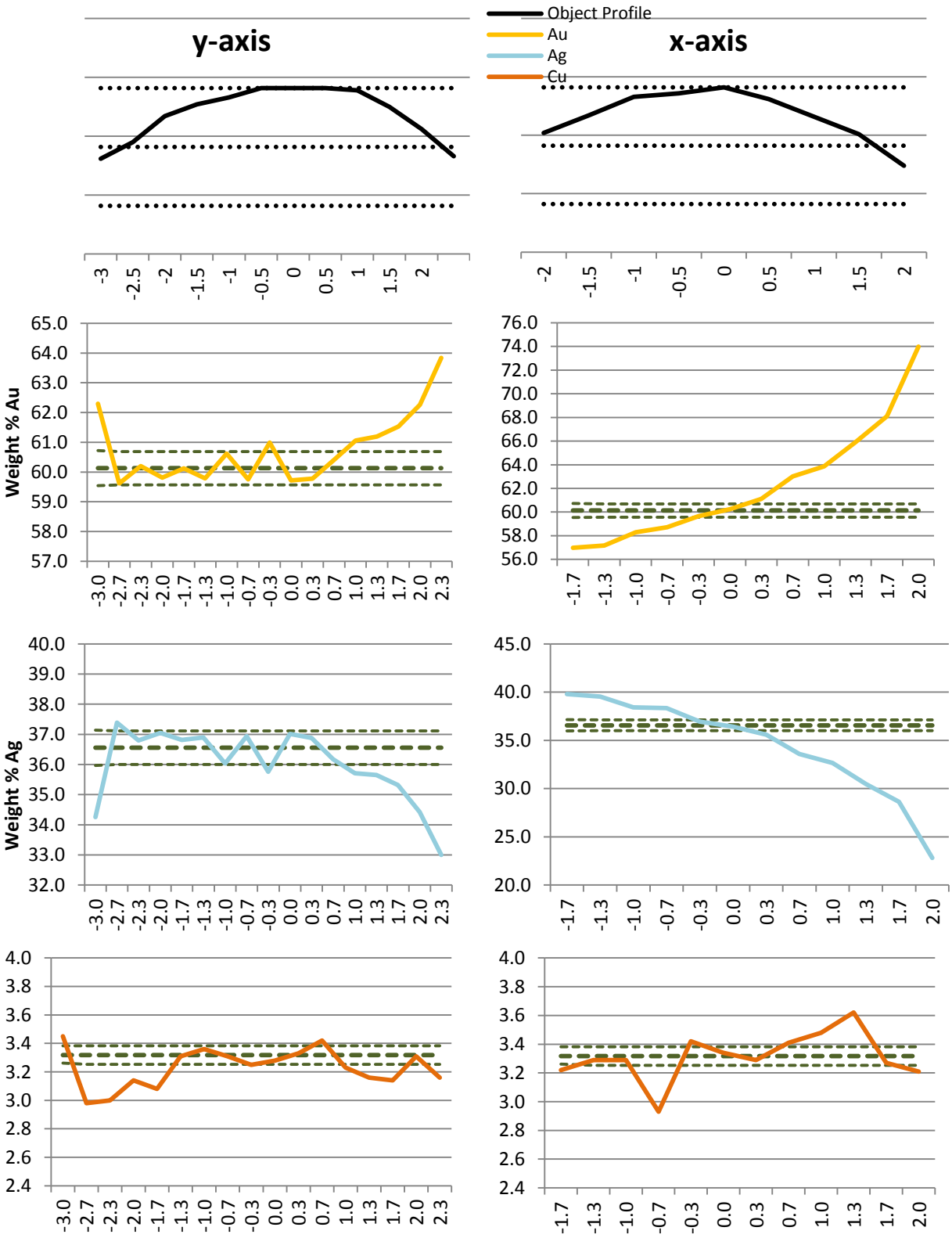

Figure 23. Graphs showing the SEM-EDX results for concentrations of gold, silver and copper as the angle of the object surface (seen in the top chart) and therefore the take-off angle in relation to the position of the detector change. The dashed lines on the graph illustrating the topography of the object show the 10 mm, 15 mm and 20 mm working distances. The thick dashed line is the average of five analyses at the flat top of K88, and the thinner dashed lines show the standard deviation from this average.

References

Araújo, M.F., Alves, L.C. and Cabral, J.M.P., 1993. *Comparison of EDXRF and PIXE analysis of ancient gold coins*. Nuclear Instruments and Methods in Physics Research **75**, 450-453.

Bachmann, H.G., 1995. Gold Analysis: From fire assay to spectroscopy - a review. In Morteani, G., Northover, J.P. (Eds.). *Prehistoric Gold in Europe: Mines, Metallurgy and Manufacture*, Kluwer Academic Publishers Dordrecht, pp. 303-315.

Blakelock, E., forthcoming. Comparison between the results from Paris PIXE, Birmingham XRF and the British Museum XRF and SEM-EDX. British Museum, London. Science Report PR07444-11. [2016 - see now Staffordshire Hoard Research Report 22]

Cowell, M., 1977. *Energy dispersive X-ray fluorescence analysis of ancient gold alloys*. PACT Journal of the European study group on physical, chemical and mathematical techniques applied to archaeology **1**, 76-85.

Cowell, M., 1998. Coin analysis by energy dispersive X-ray Fluorescence Spectrometry. In Oddy, W.A., Cowell, M. (Eds.). *Metallurgy in numismatics*, Royal Numismatic Society, London, pp. 448-460.

Cowell, M. and Hook, D.R., 2010. Analysis of the metal artefacts. In Johns, C. (Ed.). *The Hoxne Late Roman Treasure*, British Museum Press, London, pp. 175-184.

Craddock, P.T., 2000. Historical survey of gold refining: Surface treatments and refining worldwide, and in Europe prior to AD 1500. In Ramage, A., Craddock, P.T. (Eds.). *King Croesus' Gold: Excavations at Sardis and the history of gold refining*, The British Museum Press, London, pp. 27-53.

Dugmore, J.M.M. and DesForges, C.D., 1979. *Stress corrosion in gold alloys*. Gold Bulletin **12**, 140-144.

Forty, A.J., 1979. *Corrosion micromorphology of noble metal alloys and depletion gilding*. Nature **282**, 597-598.

Forty, A.J., 1981. *Micromorphology studies of the corrosion of gold alloys*. Gold Bulletin **14**, 25-35.

German, R.M., 1981. *The role of microstructure in the tarnish of low-gold alloys*. Metallography **14**, 253-266.

Goldstein, J., Newbury, D., Joy, D., Lyman, C., Echlin, E., Sawyer, L. and Michael, J., 2003. *Scanning Electron Microscopy and X-Ray Microanalysis*. 3rd ed. Kluwer Academic, New York.

Hall, E.T., 1961. *Surface enrichment of buried metals*. Archaeometry **4**, 61-66.

Heginbotham, A., Bezur, A., Bouchard, M., Davis, J.M., Eremin, K., Frantz, J.H., Glinsman, L., Hayek, L.-A., Hook, D.R., Kantarelou, V., Karydas, A.G., Lee, L., Mass, J., Matsen, C., McCarthy, B., McGath, M., Shugar, A., Sirois, J., Smith, D. and Speakman, R.J., 2011. Bringing context to the Smithsonian collections of Pre-Columbian gold from Panama through technical examination and analysis. In Mardikian, P., Chemello, C., Watters, C., Hull, P. (Eds.). *Metal 2010, Proceedings of the Interim Meeting of the ICOM-CC Metal Working Group, Charleston, South Carolina, USA,11-15 October 2010* Clemson University, South Carolina, pp. 266-272.

Hook, D.R. and Needham, S.P., 1989. *A comparison of recent analyses of British Late Bronze Age goldwork with Irish parallels*. Jewellery Studies **3**, 15-24.

Kallithrakas-Kontos, N. and Katsanos, A.A., 1998. PIXE analysis of ancient coins. In Oddy, W.A., Cowell, M. (Eds.). *Metallurgy in numismatics*, Royal Numismatic Society, London, pp. 461-471.

La Niece, S., 1995. *Depletion gilding from third millennium B.C. Ur*. Iraq **57**, 41-47.

Lehrberger, G. and Raub, C.J., 1995. A look into the interior of Celtic gold coins. In Morteani, G., Northover, J.P. (Eds.). *Prehistoric Gold in Europe: Mines, Metallurgy and Manufacture*, Kluwer Academic Publishers Dordrecht, pp. 341-355.

Letchman, H., 1973. The gilding of metals in pre-Columbian Peru. In Young, W.J. (Ed.). *Application of science in examination of works of art: Proceedings of the seminar June 15-19, 1970*, Museum of Fine Art, Boston, pp. 38-52.

Möller, P., 1995. Electrochemical corrosion of natural gold alloys. In Morteani, G., Northover, J.P. (Eds.). *Prehistoric Gold in Europe: Mines, Metallurgy and Manufacture*, Kluwer Academic Publishers Dordrecht, pp. 356-367.

Mongiatti, A., Meeks, N. and Simpson, S.J., 2010. A gold four-horse model chariot from the Oxus Treasure. A fine illustration of Achaemenid goldwork. In Saunders, D. (Ed.). *The British Museum Technical Research Bulletin **4***, Archetype Publications, London, pp. 27-38.

Northover, J.P., 1998. Analysis in the electron microprobe and scanning electron microscope. In Oddy, W.A., Cowell, M. (Eds.). *Metallurgy in numismatics*, Royal Numismatic Society, London, pp. 94-113.

Ogden, J., 1977. *Platinum group metal inclusions in ancient gold artifacts*. Historical Metallurgy Journal **11**, 53-72.

Pingel, V., 1995. Technical aspects of prehistoric gold objects on the basis of material analysis. In Morteani, G., Northover, J.P. (Eds.). *Prehistoric Gold in Europe: Mines, Metallurgy and Manufacture*, Kluwer Academic Publishers Dordrecht, pp. 385-398.

Raub, C.J., 1995. Metallurgy of gold and silver in prehistoric times. In Morteani, G., Northover, J.P. (Eds.). *Prehistoric Gold in Europe: Mines, Metallurgy and Manufacture*, Kluwer Academic Publishers Dordrecht, pp. 243-259.

Scott, D.A., 1983a. *Depletion gilding and surface treatment of gold alloys from the Nariño area of ancient Colombia*. Historical Metallurgy Journal **17**, 99-115.

Scott, D.A., 1983b. *The Deterioration of Gold Alloys and Some Aspects of Their Conservation*. Studies in Conservation **28**, 194-203.

Stern, W.B., 1995. On non-destructive analysis of gold objects. In Morteani, G., Northover, J.P. (Eds.). *Prehistoric Gold in Europe: Mines, Metallurgy and Manufacture*, Kluwer Academic Publishers Dordrecht, pp. 317-328.

Tate, J., 1986. *Some problems in analysing museum material by nondestructive surface sensitive techniques*. Nuclear Instruments and Methods in Physics Research **14**, 20-23.

Untracht, O., 1982. *Jewelry Concepts and Technology*. Robert Hale, London.

Verma, H.R., 2007. *Atomic and nuclear analytical methods* Springer, Berlin.

Voute, A., 1995. Some experiences with the analysis of gold objects. In Morteani, G., Northover, J.P. (Eds.). *Prehistoric Gold in Europe: Mines, Metallurgy and Manufacture*, Kluwer Academic Publishers Dordrecht, pp. 329-340.

Wise, E.M., 1948. Gold and gold alloys. In Uhlig, H.H. (Ed.). *The Corrosion Handbook*, J. Wiley & Sons, New York, pp. 112-119.

Wise, E.M., 1964. *Gold: Recovery, properties and applications*. Van Nostrand Company Ltd, London.

Staffordshire Hoard Research Reports

Staffordshire Hoard Research Reports were produced by the project

Contextualising Metal-Detected Discoveries: Staffordshire Anglo-Saxon Hoard

Historic England Project 5892

The Staffordshire Hoard is owned by the Birmingham City Council and the Stoke-on-Trent City Council and cared for on their behalf by Birmingham Museums Trust and The Potteries Museum & Art Gallery.

The Staffordshire Hoard research project was conducted by Barbican Research Associates Ltd and funded by Historic England and the owners.

Historic England

Birmingham City Council

City of Stoke-on-Trent

Barbican RA

Birmingham Museums

The Potteries & museum art gallery